

FINITE ELEMENT SIMULATION OF FRACTURE BEHAVIOUR OF NANOGLASS

M.Tech. Thesis

By

AKSHAY ANJAYYA GARDAS

2002103020



**DISCIPLINE OF MECHANICAL SYSTEM DESIGN
INDIAN INSTITUTE OF TECHNOLOGY INDORE**

MAY 2022

FINITE ELEMENT SIMULATION OF FRACTURE BEHAVIOUR OF NANOGLASS

A THESIS

*Submitted in partial fulfillment of the
Requirements for the award of the degree
Of
Master of Technology*

By

**AKSHAY ANJAYYA GARDAS
2002103020**



**DISCIPLINE OF MECHANICAL SYSTEM DESIGN
INDIAN INSTITUTE OF TECHNOLOGY INDORE
MAY 2022**



INDIAN INSTITUTE OF TECHNOLOGY INDORE

CANDIDATE'S DECLARATION

I hereby certify that the work which is being presented in the thesis entitled **FINITE ELEMENT SIMULATION OF FRACTURE BEHAVIOUR OF NANOGLASS** in the partial fulfillment of the requirements for the award of the degree of **MASTER OF TECHNOLOGY** and submitted in the **DISCIPLINE OF MECHANICAL ENGINEERING**, Indian Institute of Technology Indore, is an authentic record of my own work carried out during the time period from July 2021 to June 2022 under the supervision of **Dr. Indrasen Singh, Assistant Professor, Discipline of Mechanical Engineering.**

The matter presented in this thesis has not been submitted by me for the award of any other degree of this or any other institute.

G. Akshay

**Signature of the student with date
AKSHAY A. GARDAS**

This is to certify that the above statement made by the candidate is correct to the best of my/our knowledge.

[Signature]

01-06-2022

Signature of the Supervisor of
M.Tech. thesis (with date)
DR. INDRASEN SINGH

AKSHAY A. GARDAS has successfully given his/her M.Tech. Oral Examination held on **24 MAY 2022.**

[Signature]

01-06-2022

Signature(s) of Supervisor(s) of M.Tech. thesis
Date:

G. Vishu

Convener, DPGC
Date: 02/06/22

[Signature]

02/06/2022

Signature of PSPC Member #1
Date:

[Signature]

Signature of PSPC Member #2
Date: 2/6/2022

ACKNOWLEDGEMENTS

First, I would like to thank my M-tech thesis supervisor **Dr. Indrasen Singh**, without his guidance, it was not possible for me to complete this work. He helped me a lot whenever I ran into a trouble spot or any other problems with implementation and research work. Discussions with him have always been educative. I have learned lot of things during my project work. His guidance was valuable. He inspired and motivated me in all the walks of this work. He never fails to help his students in general even after being loaded with so much administrative works. I am very thankful to him in this memorable journey.

I am thankful to **Indian Government** (MHRD) for financial support and our **Director Prof. Suhas Joshi** for giving an opportunity to carry out the research work and for providing all the facilities.

I also thank my colleagues in the lab **Mr. Ramanand Dadhich, Mr. Hirmukhe Sidaram, Mr. Eli Pradeep, Mr. Nischay Saurabh, Mr. Nagendra Ranawat** and **Mr. Sumit Chorma** for their helpful suggestions time to time. Special thanks to Ramanand sir and Hirmukhe sir for his help. His excellence and knowledge in the field of experimental and Simulation works helped me a lot.

My special thanks go to **my parents and my brother** for their full support and encouragement.

AKSHAY A. GARDAS

M-Tech (Mechanical System Design)

Department of Mechanical Engineering

IIT Indore

Abstract

In this study our main is to understand how differently the nanoglass behaves under mixed mode loading condition, firstly if we change in Notch radius with keeping average grain size constant and secondly change in average grain size with keeping Notch size constant. We performed simulation under condition of 2D plane strain, small scale yielding (SSY) using Anand-Su model. It is observed that the As Radius of notch to average grain size ratio is increasing the volume fraction in yielding is decreasing in case of Effect of Notch size and almost remains constant in case of Effect of Grain size, shear band pattern is diffused in the Nanoglass.

TABLE OF CONTENTS

LIST OF TABLES

LIST OF FIGURES

Chapter 1: Introduction

1.1 General introduction	(1)
1.2 Production of Nanoglass.....	(3)
1.2.1 Inert Gas Condensation.....	(3)
1.2.2 Magnetron sputtering.....	(3)
1.3 Literature Review.....	(4)
1.4 Problem Statement.....	(5)
1.5 Issues to be addressed.....	(6)
1.6 Objectives.....	(6)

Chapter 2: Constitutive Model

Chapter 3: Modeling and Analysis aspects

3.1 Modeling and Analysis aspects for the Effect of Notch Size	(10)
3.2 Modeling and Analysis aspects for the Effect of Grain Size.....	(11)

Chapter 4: Material Parameters and Fracture Simulation aspects

Chapter 5: Results and discussion

5.1 Results and discussion for the Effect of Notch size.....	(19)
---	------

5.1.1 Discussion of Contour Plots of Logarithmic Plastic strain.....	(19)
5.1.2 The effect of M^e on the Evolution of Plastic Zone size in Nanoglass.....	(26)
5.1.3 Effect of Mode Mixity on Plastic zone size [maximum length of shear band] in Nanoglass.....	(29)
5.1.4 Mean and Standard Deviation value of Logarithmic Plastic Strain [$\log\lambda_1^p$].....	(33)
5.2 Results and discussion for the Effect of Average Grain size	(39)
5.2.1 Discussion of Contour Plots of Logarithmic Plastic strain.....	(39)
5.2.2 The effect of M^e on the Evolution of Plastic Zone size in Nanoglass.....	(47)
5.2.3 Effect of Mode Mixity on Plastic zone size [maximum length of shear band] in Nanoglass.....	(48)
5.2.4 Mean and Standard Deviation value of Logarithmic Plastic Strain [$\log\lambda_1^p$].....	(52)
Chapter 6: Conclusion and future work	
6.1 Conclusion and Future work	(57)
References.....	(59)

List of tables

Table 1: No. of nodes and elements for the Effect of Notch size.....	(14)
Table 2: No. of nodes and elements for the Effect of Grain size	(14)
Table 3: Stress intensity factor for given M^e values.....	(16)
Table 4: Material Properties taken for Simulations.....	(17)

List of figures

- Figure 1.1: Comparison of the diffusivities in Nanocrystalline (nc) Cu, Ni and Pd in comparison to the diffusivities in single crystals (SC) of Cu, Ni and Pd. T_m is the absolute melting temperature (2)
- Figure 1.2: Work-hardening rate of (Al-1.6 at % Cu) crystals at room temperature after a solution treatment, water quenching, and aging at 190 °C for various times. The strain rate of the deformation process was $3 \times 10^{-4} \text{ s}^{-1}$. The aging at 190 °C results in a two-phase material consisting of precipitates embedded in a crystalline solid solution..... (2)
- Figure 2: Production of Nanoglasses by consolidation on nanometer-sized glassy clusters produced by inert-gas condensation..... (3)
- Figure 3: Finite Element Model..... (9)
- Figure 4: Finite Element Modelling for the Notch Size $[R] = 0.5, 13, 30 \text{ nm}$ and Average Grain Size $[d] = 10 \text{ nm}$ (10)
- Figure 5: Finite Element Modelling for the Average Grain Size $[d] = 5, 10, 20 \text{ nm}$ Notch Size $[R] = 13 \text{ nm}$ (12)
- Figure 6: In Plane displacement applied on outer nodes of circular domain..... (15)
- Figure 7: contour plots of Logarithmic Plastic Strain $[\log \lambda_1^p]$ for the corresponding M^e values for the Notch Size $[R] = 0.5 \text{ nm}$ and Average Grain Size $[d] = 10 \text{ nm}$ (20)

Figure 8: Contour plots of Logarithmic Plastic Strain [$\log\lambda_1^p$] for the corresponding M^e values for the Notch Size [R] = 13 nm and Average Grain Size [d] = 10 nm..... (22)

Figure 9: contour plots of Logarithmic Plastic Strain [$\log\lambda_1^p$] for the corresponding M^e values for the Notch Size [R] = 30 nm and Average Grain Size [d] = 10 nm (24)

Figure 10: Variation of volume fraction [v_f^y] of material undergoing in plastic yielding with increase in loading factor for corresponding M^e values..... (28)

Figure 11: Variation of Plastic Zone size [maximum length of Shear Band] with increase in loading factor [|K|] for corresponding M^e values and Notch Size [R]= 0.5, 13, 30 nm, Average Grain Size [d] = 10 nm..... (30)

Figure 12: Variation of Plastic Zone size [maximum length of Shear Band] with increase in loading factor [|K|] for Notch Size [R]= 0.5, 13, 30 nm, Average Grain Size [d] = 10 nm and corresponding M^e values(31)

Figure 13: Variation of Mean value of Logarithmic Plastic strain [$\log\lambda_1^p$] with increase in loading factor [|K|] for Notch Size [R] = 0.5, 13, 30 nm, Average Grain Size [d] = 10 nm and for corresponding M^e values..... (34)

Figure 14: Variation of Standard Deviation value of Logarithmic Plastic strain [$\log\lambda_1^p$] with increase in loading factor [|K|] for Notch Size [R] = 0.5, 13, 30 nm, Average Grain Size [d] = 10 nm and for corresponding M^e values (36)

Figure 15: Contour plots of Logarithmic Plastic Strain [$\log\lambda_1^p$] for the corresponding M^e values for the Average Grain Size [d] = 5 nm and Notch Size [R] = 13..... (40)

Figure 16: Contour plots of Logarithmic Plastic Strain [$\log\lambda_1^p$] for the corresponding M^e values for the Average Grain Size [d] = 10 nm and Notch Size [R] = 13 nm..... (42)

Figure 17: Contour plots of Logarithmic Plastic Strain [$\log\lambda_1^p$] for the corresponding M^e values for the Average Grain Size [d] = 20 nm and Notch Size [R] = 13 (44)

Figure 18: Variation of volume fraction [v_f^y] of material undergoing in plastic yielding with increase in loading factor for corresponding M^e values (47)

Figure 19: Variation of Plastic Zone size [maximum length of Shear Band] with increase in loading factor [K] for corresponding M^e values and Average Grain Size [d] = 5, 10, 20 nm, Notch Size [R]= 13 nm..... (49)

Figure 20: Variation of Plastic Zone size [maximum length of Shear Band] with increase in loading factor [K] for corresponding M^e values and Average Grain Size [d] = 5, 10, 20 nm, Notch Size [R]= 13 nm..... (50)

Figure 21: Variation of Mean value of Logarithmic Plastic strain [$\log\lambda_1^p$] with increase in loading factor [K] for Average Grain Size [d] = 5, 10, 20 nm Notch Size [R] = 13 nm, and for corresponding M^e values..... (53)

Figure 22: Variation of Standard Deviation value of Logarithmic Plastic strain [$\log\lambda_1^p$] with increase in loading factor [K] for Average Grain Size [d] = 5, 10, 20 nm, Notch Size [R] = 13 nm, and for corresponding M^e values..... (55)

Chapter-1

Introduction

1.1 General introduction

Most of the metal which we are using in daily need from the human life began are crystalline materials. In the age of stone peoples were quartz and granite for making his tools for hunting of animals. Now a days light weight metal, high strength alloy, superconductors, ferroelectrics, special ferromagnetic materials, semiconductors (e.g., Si) are used widely. From the age of stone to recent time crystalline materials are used widely. This is the reason over the past few years most of researcher is working on amorphous metallic alloys or metallic glasses through which he came upto Nanoglass (NG) to fulfil industrial and commercial requirement. In 1989, the fundamental notion of Nanoglass was proposed in the first publication on the subject. The goal was to see if planar flaws or interfaces might be eliminated. This would result in a new class of metallic spectacles being introduced. Amorphous materials with new structural characteristics in addition to new properties Following the same pattern compacting and processing synthesis and processing route sintering nanoparticles to form Nano crystalline materials Gleiter proposed that amorphous matter be consolidated.

The fundamental reason for choosing crystalline materials is that their properties can be changed or controlled by changing their defect microstructures and/or chemical microstructures. Figure 1.1 shows how changing the defect microstructure by providing an incoherent interface with high density can dramatically improve the Cu, Ni, and Pd metals diffusivities. Figure 1.2 shows how changing the chemical microstructure of a substance can change its properties [2].

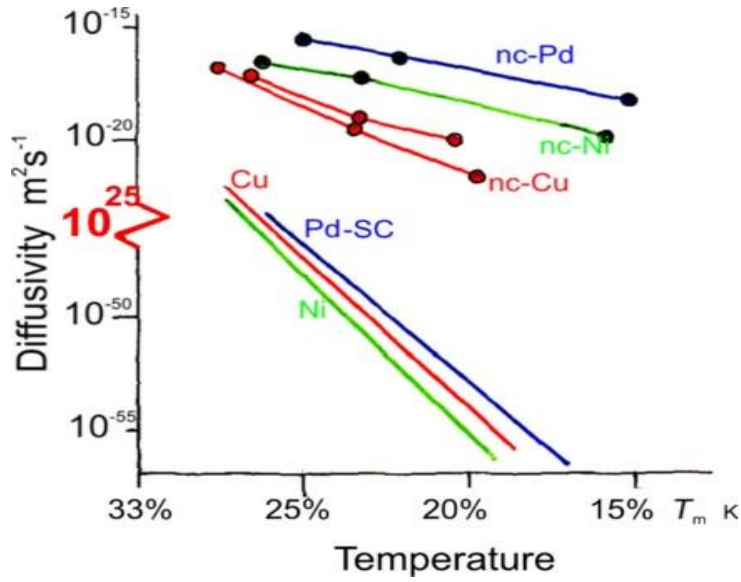


Fig. 1.1- Comparison of the diffusivities in Nanocrystalline (nc) Cu, Ni and Pd in comparison to the diffusivities in single crystals (SC) of Cu, Ni and Pd. T_m is the absolute melting temperature

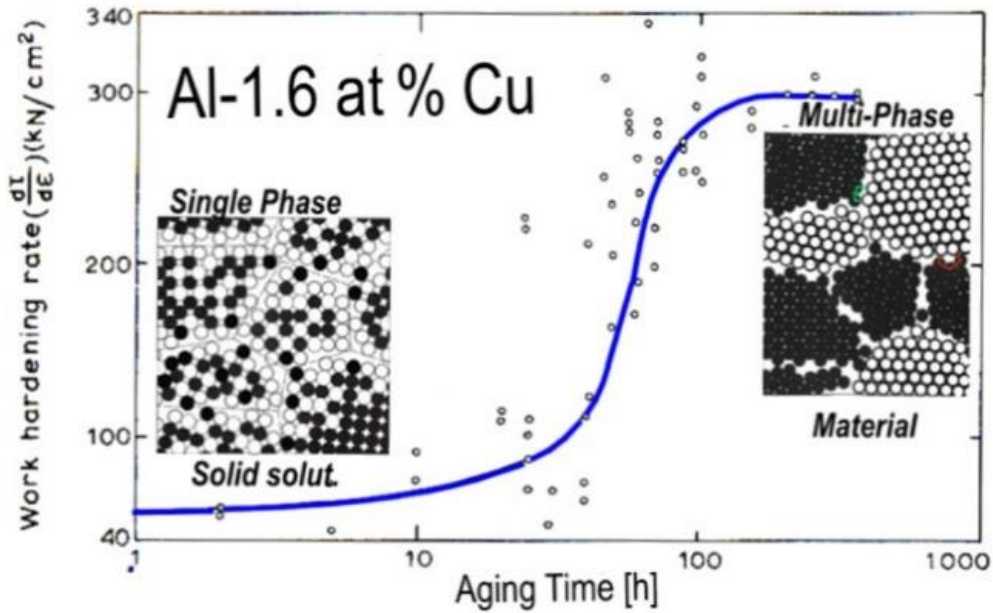


Fig. 1.2- Work-hardening rate of (Al-1.6 at % Cu) crystals at room temperature after a solution treatment, water quenching, and aging at 190 °C for various times. The strain rate of the deformation process was $3 \times 10^{-4} \text{ s}^{-1}$. The aging at 190 °C results in a two-phase material consisting of precipitates embedded in a crystalline solid solution

1.2 Production of Nanoglass

So far, Nanoglass has been produced in the following three ways:

1.2.1 Inert-gas condensation

Inert-gas condensation is one method for making Nanoglass (Figure 2). The next two processes make up this production procedure. Evaporating (or sputtering) the material in an inert gas atmosphere produces nanometer-sized glassy clusters in the first step. The resultant clusters are then compacted into a pellet-shaped Nanoglass under pressures of up to 5 GPA. Inert gas condensation has been used to make Nanoglass from a range of alloys which including Au–Si, Au–La, Cu–Sc, Fe–Sc, Fe–Si, La–Si, Pd–Si, Ni–Ti, Ni–Zr, and Ti–P [2].

1.2.2 Magnetron sputtering

So far, this approach has only been used on Au-based metallic glasses. Glassy areas with an average size of roughly 30 nm were formed in the Nanoglass. The latest studies on the properties and structure of Nanoglass created by magnetron sputtering reveal that they are similar to Nanoglass made by inert gas condensation method in structure and properties [2].

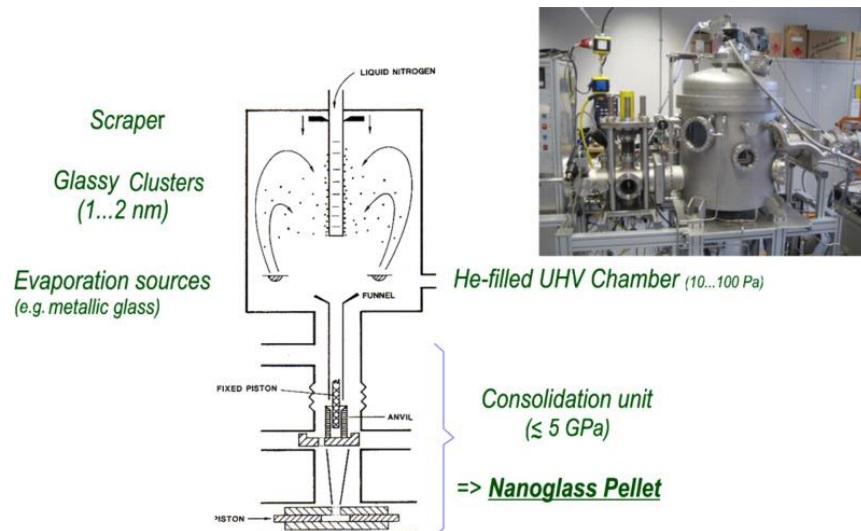


Fig. 2- Production of Nanoglasses by consolidation on nanometer-sized glassy clusters produced by inert-gas condensation

1.3 Literature Review

Xiao Lei Wang et al. [11] performed Nanoindentation tests and quantitative in a transmission electron microscope to analyse Plasticity property of a Nanoglass which is scandium-based. In this paper, it is observed that the Nanoglass has a much improved ability to deform plastically as compared to Metallic glass. The primary deformation mode is due to multiple shear band development, which varies from monolithic MG with similar chemical composition. The deformation of Nanoglass is occurred more uniformly with multiple shear bands whereas in MG deformation is occurred catastrophically.

L. Anand et. al [4] studied a Coulomb–Mohr type constitutive theory for amorphous viscoplastic material and finite-deformation in detailed manner. It is implemented in finite element programme which specifically used to study the deformation behaviour metallic glass of amorphous structure in strip bending, indentation, compression, tension.

Parag Tandaiya et al. [8] studied deformation behaviour of amorphous material such as metallic glass under Mode I loading condition by performing finite element simulation under 2D plane strain and small scale yielding condition. The continuum elastic–viscoplastic constitutive theory is applied in this study. The shear band pattern obtained from the simulation results are qualitatively matches with experimental results.

S. S. Hirmukhe et. al [1] studied a fracture behaviour of Nanoglass and for Notch size of 0.5 nm under the Mode mixity parameter (M_e) of 0, 0.25, 0.75, 1 with 2D plane strain and small scale yielding condition. A finite deformation, Mohr-Coloumb type plasticity model for Metallic Glass recommended by Anand and Su (2005) is applied in this study. Deformation of Nanoglass is retarded with increase in mode mixity parameter is observed in this study.

Sha et. al [10] study is focused on the deformation behaviour of Nanoglass [notch size = 2.5, 5, 15, 20 nm, Average grain size = 10nm] samples under pure mode – I loading condition using MD simulation.

1.4 Problem Statement

A huge amount of efforts already been taken to understand the deformation behaviour of Nanoglass under tensile, compressive, indentation loading. Some of the studies had been done to understand fracture behaviour of Nanoglass (NGs). One of the other study is focused on the fracture behaviour of Nanoglass [Notch size= 0.5 nm, Average grain size = 10nm] and metallic glass under pure mode - I,II and mixed mode loading condition using commercially available finite element program Abaqus 2017 [1]. In Notched specimen Notch is one of the main reason of stress concentrations in engineering components which playing important roles throughout safety designing. The study of notch effect is important for assessing the sensitivity of materials to notches, holes, grooves or alternative geometrical discontinuities as well as Notch size is also effects on the initiation of crack and behaviour of fracture etc. so it is necessary to do detailed study on fracture behaviour of specimen for different notch size with constant grain size under pure mode - I,II and mixed mode loading condition. Hence, two dimensional, plane strain, finite element analysis on the Specimen with Notch size (R) = 0.5, 13, 30 nm, constant Average grain size = 10 nm subjected to mixed mode

(I and II) carried out under the condition of small scale yielding (SSY) by applying constitutive model of metallic glass.

1.5 Issues need to be addressed

1. How does the Logarithmic Plastic strain $[\log\lambda_1^p]$ distribution near the notch vary for different values of the mode mixity parameter along with condition of variation in Notch Radius and keeping constant Average grain size in Nanoglass?
2. How does the Logarithmic Plastic strain $[\log\lambda_1^p]$ distribution near the notch vary for different values of the mode mixity parameter along with condition of variation in Average grain size and keeping constant Notch Radius in Nanoglass?

1.6 Objectives

- ❖ To perform finite element simulations with condition of small scale yielding (SSY) on Nanoglass with varying Notch Size and keeping constant Average Grain size to understand the crack tip mechanism under conditions of mixed mode and pure mode loading.
- ❖ To perform finite element simulations with condition of small scale yielding (SSY) on Nanoglass with varying Average Grain size and keeping constant Notch Size to understand the crack tip mechanism under conditions of mixed mode and pure mode loading.
- ❖ To study variation of the Logarithmic Plastic strain $[\log\lambda_1^p]$ distribution near the notch with mode-mixity and pure mode for all above cases.

Chapter – 2

Constitutive Model

Anand and Su et al. [4] suggested a finite deformation Mohr-Coulomb type Visco-plasticity model for metallic glass, which has been demonstrated to match the deformation behaviour of Metallic glass under bending, compression, tension, and indentation. This model presuppose that plastic deformation occurred in amorphous metals is accompanied by plastic shearing dilatation in six hypothetical slip systems specified in terms of the major axes of rotation of Kirchhoff stress. The plastic shear strain in a α^{th} slip system evolves according to this model.

$$\dot{\gamma}^{(\alpha)} = \dot{\gamma}_0 \left\{ \frac{\tau^{(\alpha)}}{c + \mu\sigma^{(\alpha)}} \right\}^{\frac{1}{m}}$$

where

m = Strain rate sensitivity parameter

$\dot{\gamma}_0$ = Reference plastic shearing rate

μ = Internal friction coefficient

$\tau^{(\alpha)}$, $\sigma^{(\alpha)}$ = Resolved shear stress and compressive normal traction acting on slip system

c = cohesion which evolves by following expression

$$c = c_{cv} + \left(\frac{b}{e - 1} \right) \left\{ e^{\left(1 - \left(\frac{\eta}{\eta_{cv}} \right) \right)} - 1 \right\}$$

b , c_{cv} = material constant

η = current level of free volume

η_{cv} = saturation level of free volume

The free volume evolution law is given by

$$\dot{\eta} = \beta \sum_{\alpha=1}^6 \dot{\gamma}^{(\alpha)}$$

β = dilatation function which is assumed to evolve with η as

$$\beta = \frac{g_0}{e - 1} \left\{ e^{\left(1 - \left(\frac{\eta}{\eta_{cv}}\right)\right)} - 1 \right\}$$

g_0 = initial value of dilatancy parameter

By writing the user defined material subroutine UMAT in the commercially available finite element package Abaqus 2017, this model was implemented. The integration of the constitutive equations is carried by the implicit backward Euler approach. In this study above mentioned model is used for the fracture behaviour analysis of Nanoglass.

Chapter – 3

Modeling and Analysis aspects

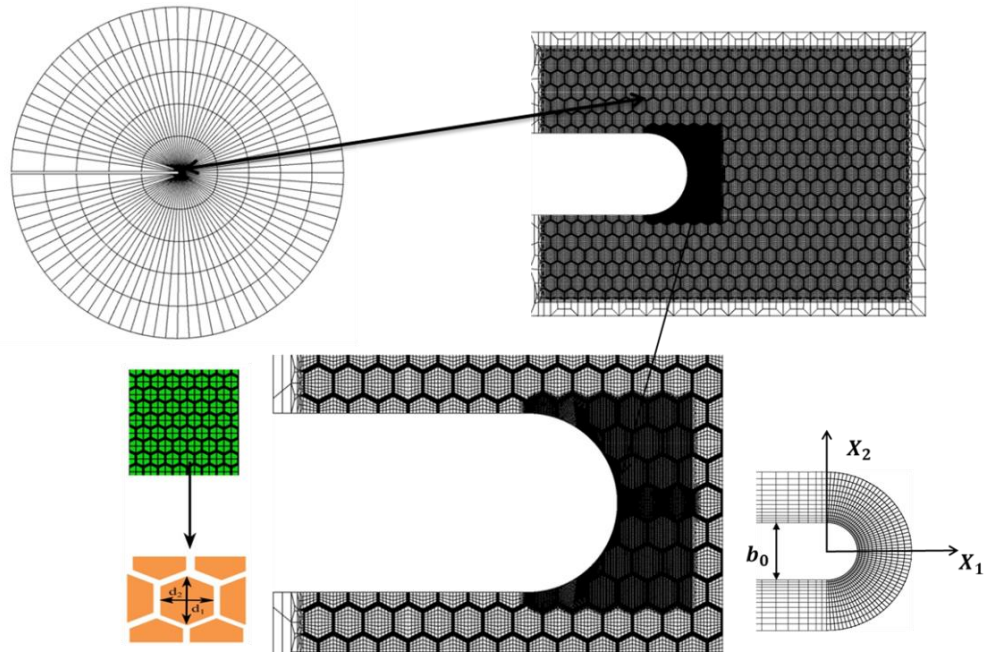


Fig. 3- Finite Element Model

This analysis is carried out by considering 2D plane strain and condition of small scale yielding (SSY). We are implementing Anand-Su model [4] in which larger circular domain with the semi-circular notch along the radius is taken up. For all cases the external outer radius of the circular domain (R_0) is maintained constant as 4000 nm. The Origin of Cartesian coordinate ($x=0, y=0$) is positioned at centre of Notch in each case. The centre of circular notch is concentric with the centre of whole circular domain in undeformed condition. The Average Grain size is the average of d_1 and d_2 distance of grain. The d_1 and d_2 are the dimensions of Hexagonal shaped glassy grain in x and y direction as shown in fig.

3.1 Modeling and Analysis for Effect of Notch Size-

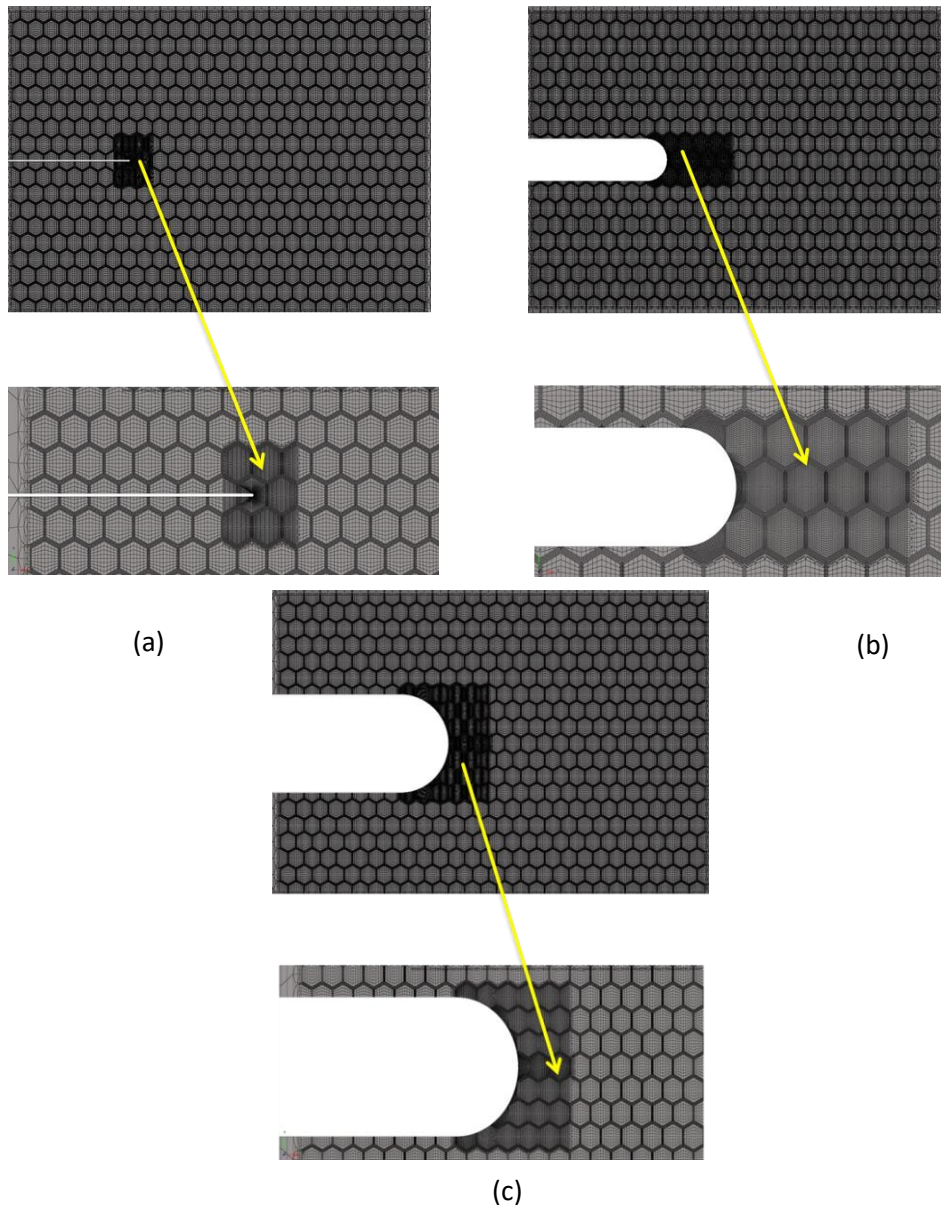
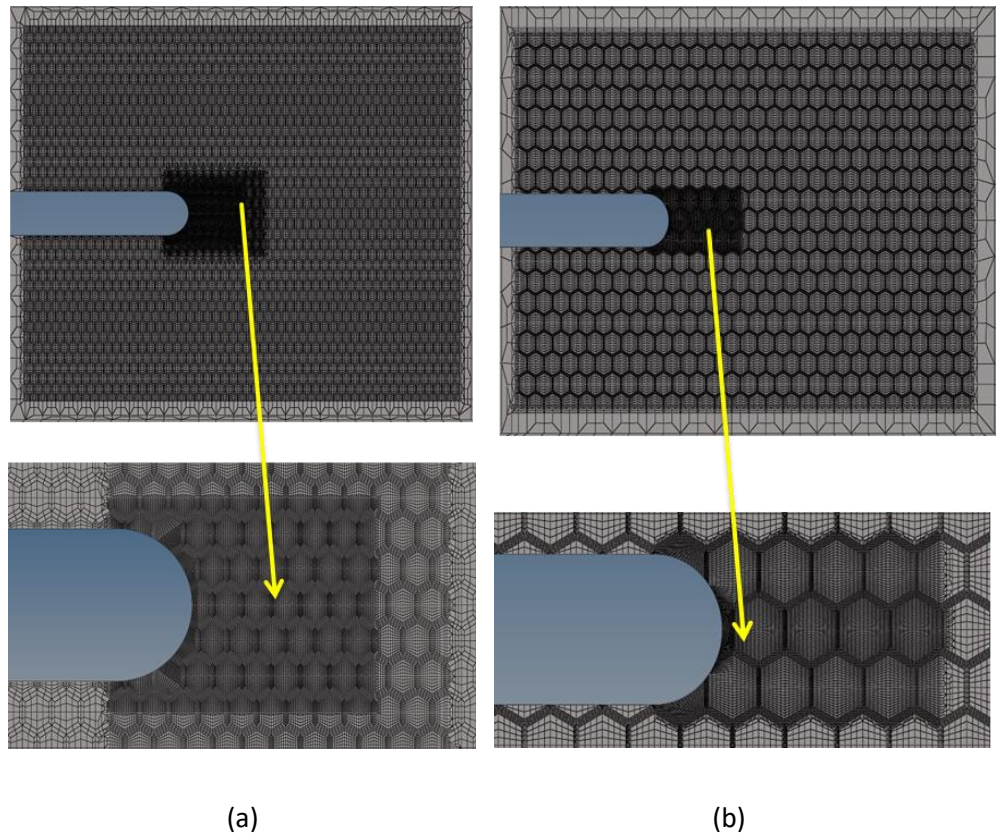


Fig. 4- Finite Element Modelling for the Notch Size $[R] = 0.5, 13, 30$ nm and Average Grain Size $[d] = 10$ nm shown in (a), (b), (c) respectively.

To understand the effect of changing notch size with grain size constant on fracture behaviour, the notch radius is taken for three cases as 0.5, 13, 30 nm and maintaining constant average grain size 10nm. The average size of Hexagonal shaped glassy grain of 10 nm is maintained by fixing $d1 = 11$

nm and $d_2 = 9$ nm in each case. The d_1 and d_2 are the dimensions of Hexagonal shaped glassy grain in x and y direction as shown in fig. The dimensions of average hexagonal glassy grain size ($d = 10$ nm) and radius of notch ($R = 0.5, 13, 30$ nm) is chosen such that its ratio of R/d is maintained as less than 1, equal to 1 and greater than 1 respectively. The size of notch ($b_0 = 2R$) is also changing with change in radius as 1, 26, 60 nm. In each case we are maintaining constant size of rectangle 261 nm \times 247 nm located in the centre of large circular domain as shown in magnified view.

3.2 Modeling and Analysis for Effect of Average Grain Size-



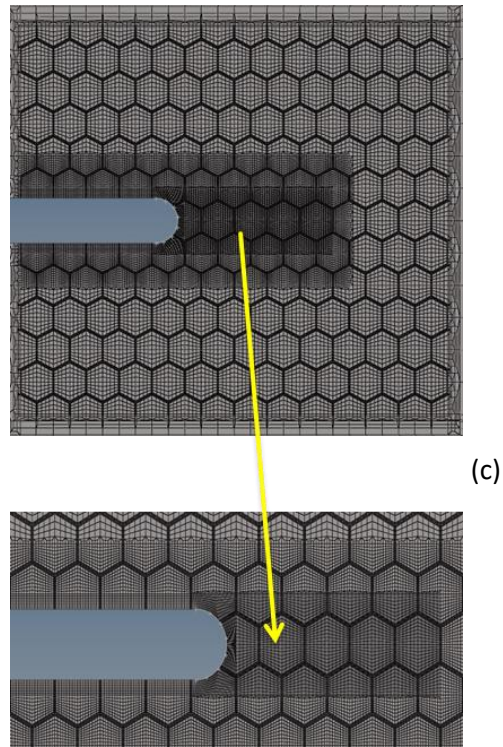


Fig. 5- Finite Element Modelling for the Average Grain Size $[d] = 5, 10, 20$ nm Notch Size $[R] = 13$ nm and shown in (a), (b), (c) respective

To understand the effect of changing Average grain size with notch size constant on fracture behaviour, the Average grain size is taken for three cases as 5, 10, 20 nm and maintaining constant average grain size 13 nm. The average size of Hexagonal shaped glassy grain of 5, 10, 20 nm is maintained by fixing $d_1 = 6, 11, 22$ nm and $d_2 = 4, 9, 18$ nm respectively. The d_1 and d_2 are the dimensions of Hexagonal shaped glassy grain in x and y direction as shown in fig. The dimensions of radius of notch ($R = 13$ nm) and average hexagonal glassy grain size ($d = 5, 10, 20$ nm) is chosen such that its ratio of R/d is maintained as greater than 1, equal to 1 and less than 1 respectively. In each case we are maintaining constant size of rectangle $261 \text{ nm} \times 247 \text{ nm}$ located in the centre of large circular domain as shown in magnified view.

Chapter-4

Material Parameters and Fracture Simulation aspects

Whole model is discretized by only four noded isoparametric quadrilateral elements. To capture the accurate fracture behaviour a highly refined mesh is implemented near notch tip. To reduce the computational time of simulation we implemented nanoglass meshing only inside the rectangle located in the centre of large circular domain and simple four noded rectangular element meshing in the remaining portion. The nanoglass meshing is consisting of hexagonal glassy grains of nanosized which are separated by interfaces. In each case interface width is maintained as 1 nm. The zoomed view of such typical hexagonal grain is shown below. For the fracture simulation the no. of elements and nodes employed for the total six different cases in both study Effect of Notch Size and Effect Average Grain Size, given in table below.

	Case 1	Case 2	Case 3
	R=0.5 nm d=10 nm $\frac{R}{d} = 0.05 < 1$	R=13 nm d=10 nm $\frac{R}{d} = 1.3 \approx 1$	R=30 nm d=10 nm $\frac{R}{d} = 3 > 1$
No. of Nodes	107538	108998	107310
No. of Elements	107290	108768	106988

Table-1- No. of nodes and elements for the Effect of Notch size

	Case 3	Case 4	Case 6
	d = 20 nm R=13 nm $\frac{R}{d} = 0.65 < 1$	d = 10 nm R= 13 nm $\frac{R}{d} = 1.3 \approx 1$	d = 5 nm R= 13 nm $\frac{R}{d} = 2.6 > 1$
No. of Nodes	41112	108998	94095
No. of Elements	40934	108768	93828

Table-2- No. of nodes and elements for the Effect of Grain size

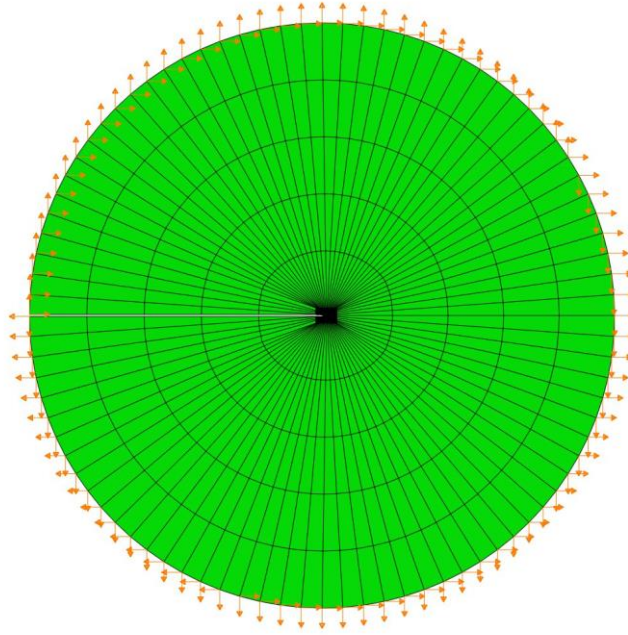


Fig. 6- In Plane displacement applied on outer nodes of circular domain.

For all the simulation, The Notch surface is considered as traction free boundary and in plane displacement (u_1 and u_2) stated by (Rice, 1968) in x and y direction respectively for condition of mixed mode (Mode I and Mode II) elastic crack tip fields are applied on external external outer boundary nodes of circular domain.

$$u_1 = \sqrt{\frac{R_0}{2\pi}} \left(\frac{1+\nu}{E} \right) \left[K_I \cos \frac{\theta}{2} \left(k - 1 + 2 \sin^2 \frac{\theta}{2} \right) + K_{II} \sin \frac{\theta}{2} \left(k + 1 + 2 \cos^2 \frac{\theta}{2} \right) \right]$$

$$u_2 = \sqrt{\frac{R_0}{2\pi}} \left(\frac{1+\nu}{E} \right) \left[K_I \sin \frac{\theta}{2} \left(k + 1 - 2 \cos^2 \frac{\theta}{2} \right) - K_{II} \cos \frac{\theta}{2} \left(k - 1 - 2 \sin^2 \frac{\theta}{2} \right) \right]$$

In the above two equation k is shear modulus which is in plain strain condition

$k = 3 - 4\mu$, where μ is poisons ratio K_I and K_{II} are the Mode I and Mode II Stress Intensity factor respectively. The loading rate is applied in small

steps ($|K|=1$ in 1 second) and effective stress intensity factor ($|K| = \sqrt{K_I^2 + K_{II}^2}$) is increasing gradually upto $|K| = 15$ while maintaining constant elastic mode mixity parameter $M^e = \frac{2}{\pi} \tan^{-1} \left(\frac{K_I}{K_{II}} \right)$ throughout the loading rate. For the computation the Elastic Mode Mixity Parameter values taken for simulations are 0, 0.25, 0.75, and 1. $M^e = 0$ is called the Pure mode II loading condition, $M^e = 1$ is called the Pure mode I loading condition and the M^e values in between 0 to 1 is called the Mixed Mode loading condition. The K_I and K_{II} Stress Intensity factor for the $|K| = 1$ for the different M^e values are given in table.

M^e	K_I	K_{II}
0	0	1
0.25	0.38269	0.92388
0.75	0.92388	0.38269
1	1	0

Table-3- Stress intensity factor for given M^e values

The loading rate and Elastic Mode Mixities values (M^e) is maintained constant for all three simulations. To induce a shear band for the study of fracture behavior we agitated the initial cohesion by 3% about its nominal value of cohesion 0.765 GPa and applied randomly to any element in meshing. The material parameters that appear in the constitutive model for Nanoglass and metallic glass of Scandium based are derived in this section, and will be used in fracture simulations in the next sections. Young's modulus (E) and initial cohesion values (Co) for Nanoglass and metallic glass are obtained from Franke et al. and Wang et al. respectively. The values of material parameters ν , μ , m , γ_0 , g_0 , n_{cv} , c_{cv} , c_{og} , c_0 are come

from Anand-Su's work and S.S. Hirmukhe work [4,1]. All the values of material parameters for Grain and interface are shown in below table.

Sr. no.	Material Property	Material Property Name	Grain	Interface
1	E	Modulus of elasticity	97	97
2	ν	Poisson's ratio,	0.36	0.36
3	μ	Internal friction coefficient,	0.08	0.25
4	γ_0	Reference plastic shear strain rate,	0.001	0.001
5	m	Strain rate sensitive parameter	0.02	0.02
6	go	Rate of dilatation parameter	0.4	0.4
7	ncv	Plastic volume at saturation,	0.005	0.005
8	Ccv	Cohesion at saturation	0.620	0.620
9	Cog(gpa)	Initial cohesion for glassy grain	0.765	----- -----
10	Co (gpa)	Initial cohesion for interface		0.670 (12.41 % lower than grain)
11	b (gpa)	Constant in cohesion function	0.145	0.05
12	b + Ccv		0.765	0.670

Table-4- Material Properties taken for simulations

Chapter-5

Result and discussion

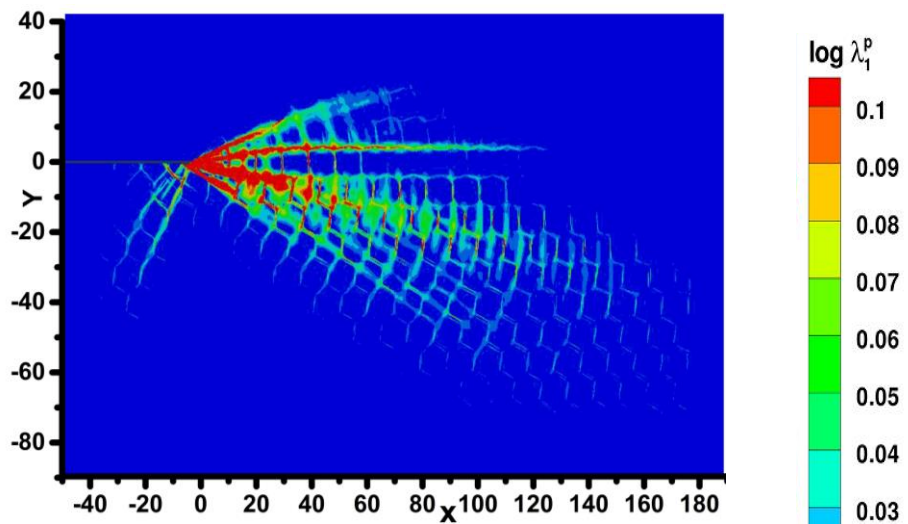
In this chapter, a result obtained in the simulations has been discussed in detail.

5.1 Results and discussion for the Effect of Notch Size-

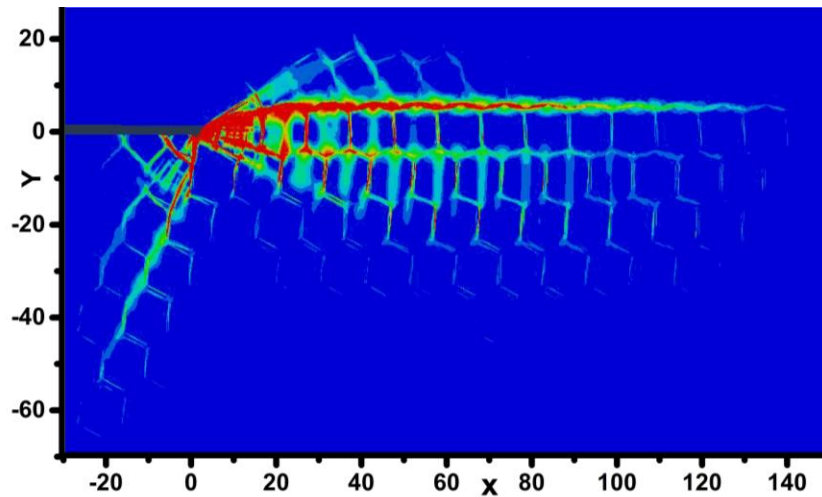
5.1.1 Discussion of Contour Plots of Logarithmic Plastic

strain

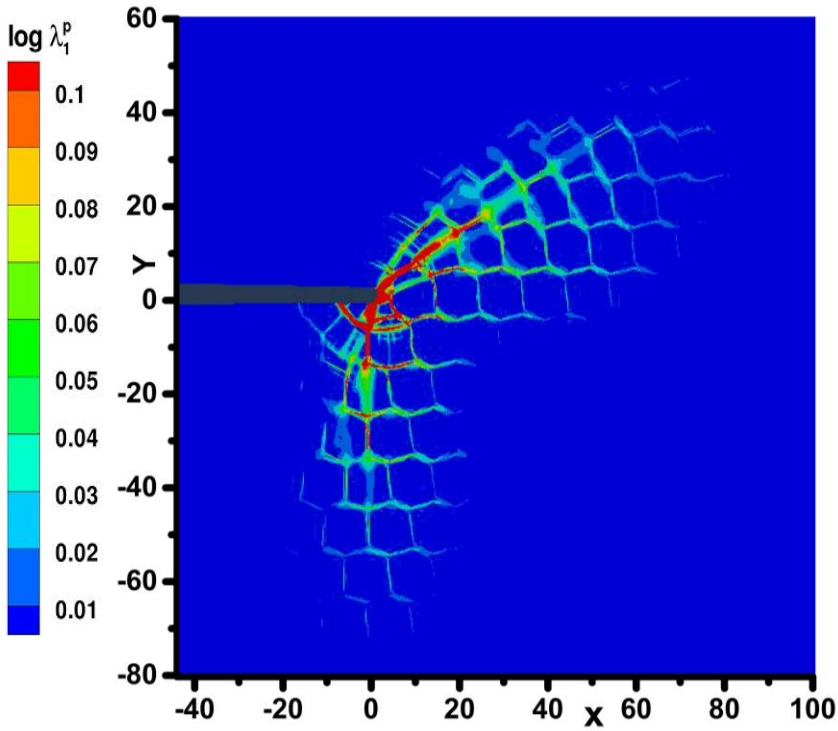
$$M^e = 0$$



$$M^e = 0.25$$



$M^e = 0.75$



$M^e = 1$

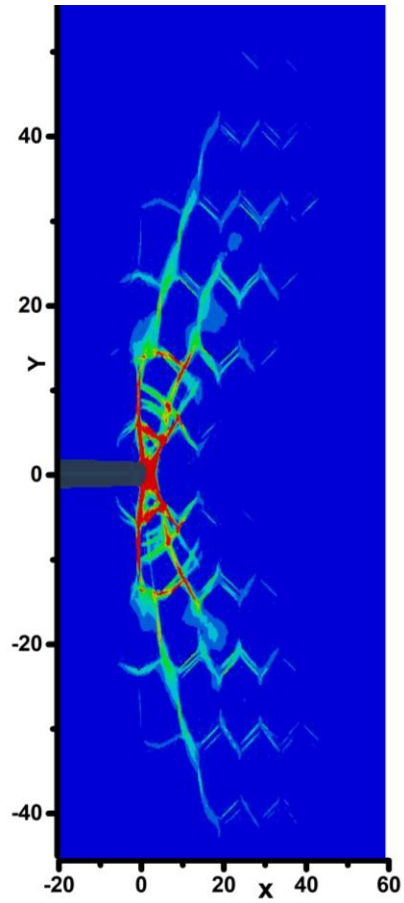
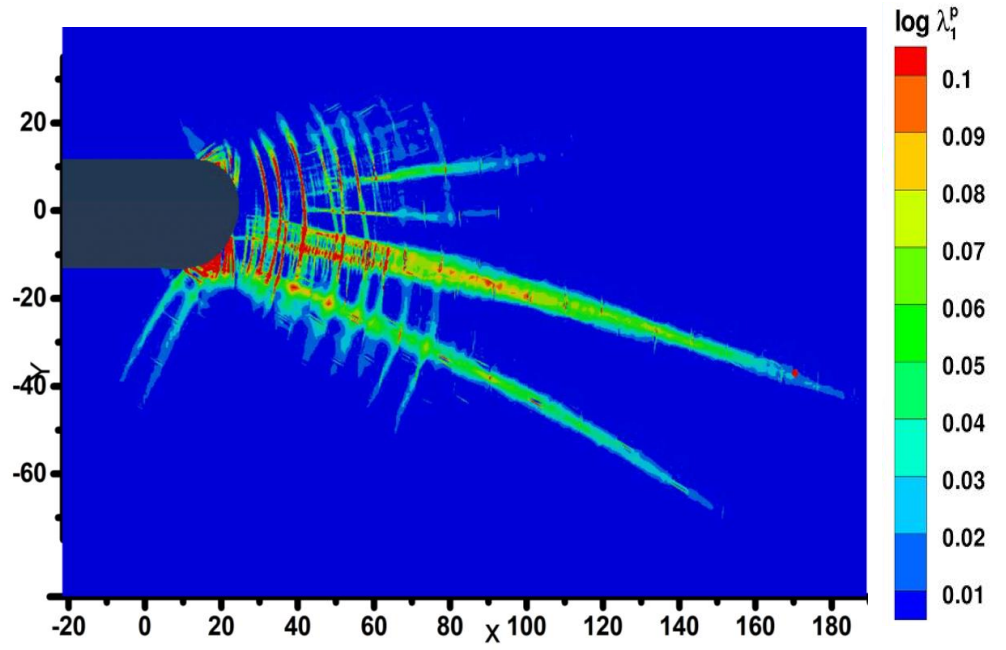
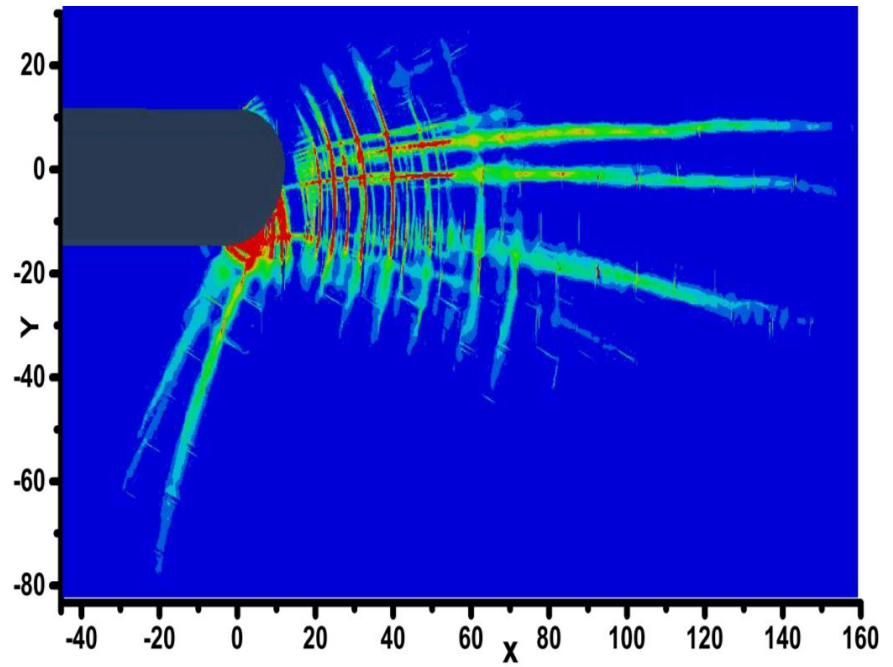


Fig. 7- contour plots of Logarithmic Plastic Strain [$\log \lambda_1^p$] for the corresponding M^e values for the Notch Size [R] = 0.5 nm and Average Grain Size [d] = 10 nm (on x and y axis in contour plots are distance up to which shear band propagating in nm in respective d

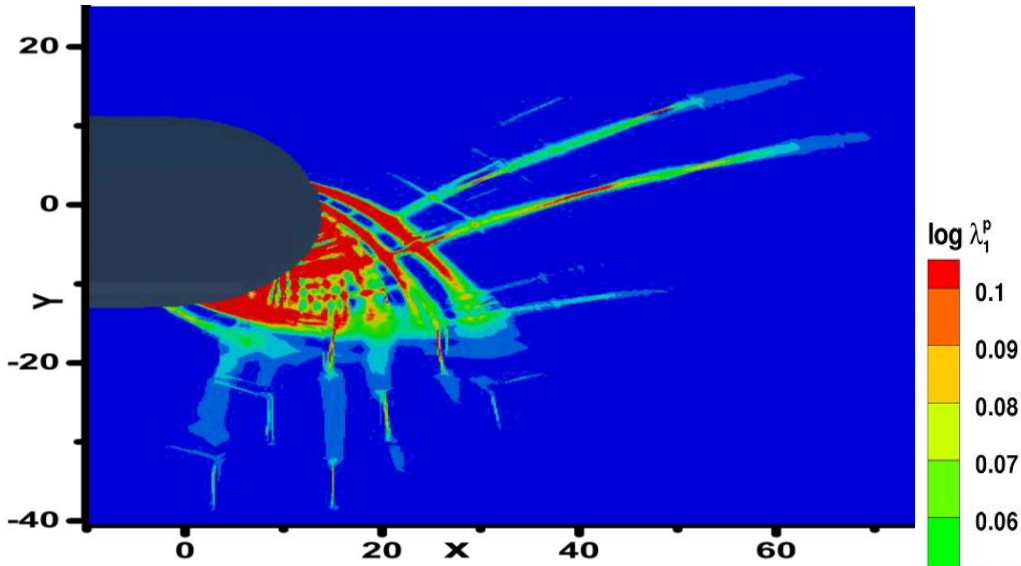
$$M^e = 0$$



$$M^e = 0.25$$



$$M^e = 0.75$$



$$M^e = 1$$

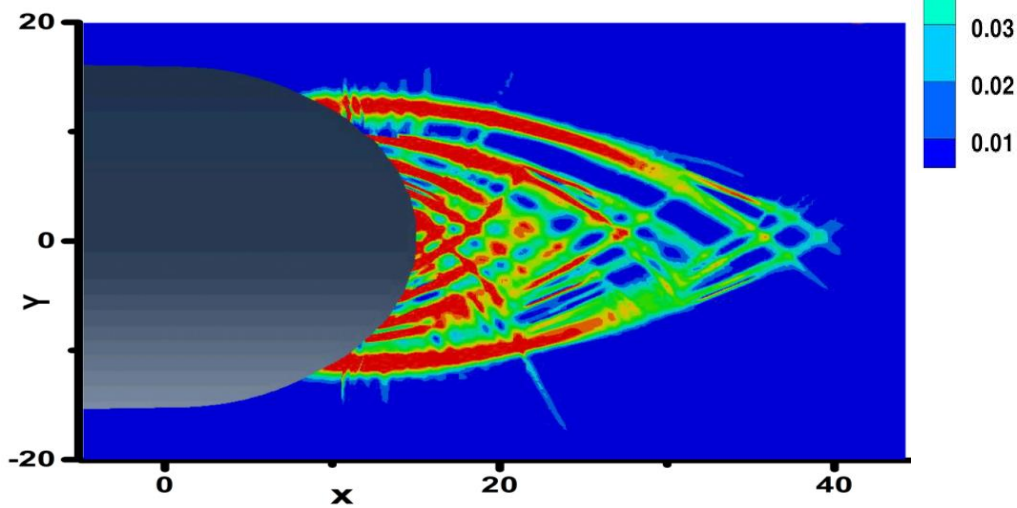
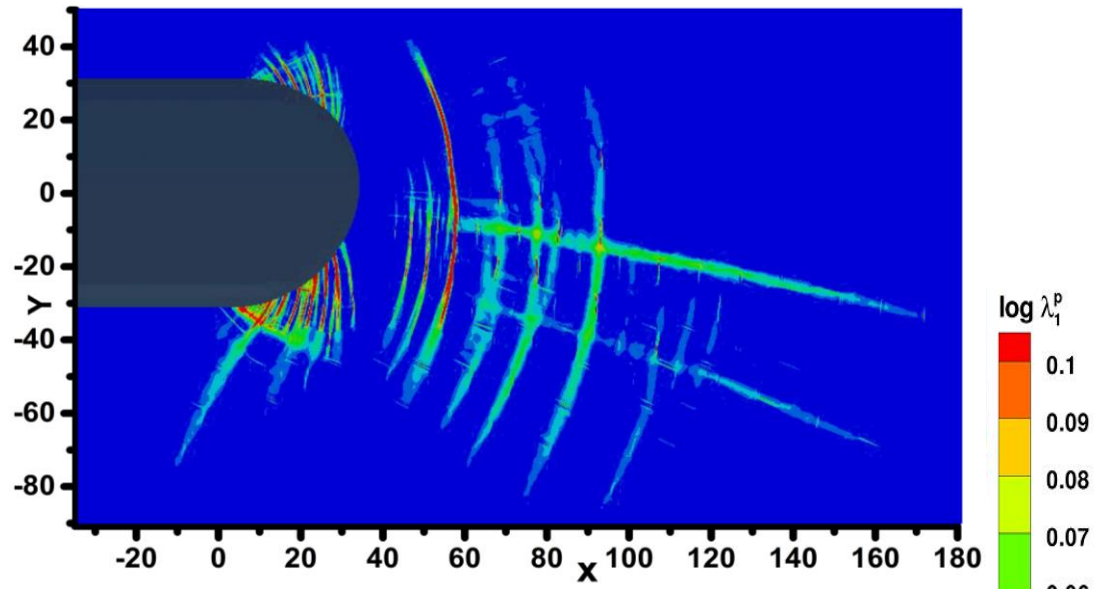
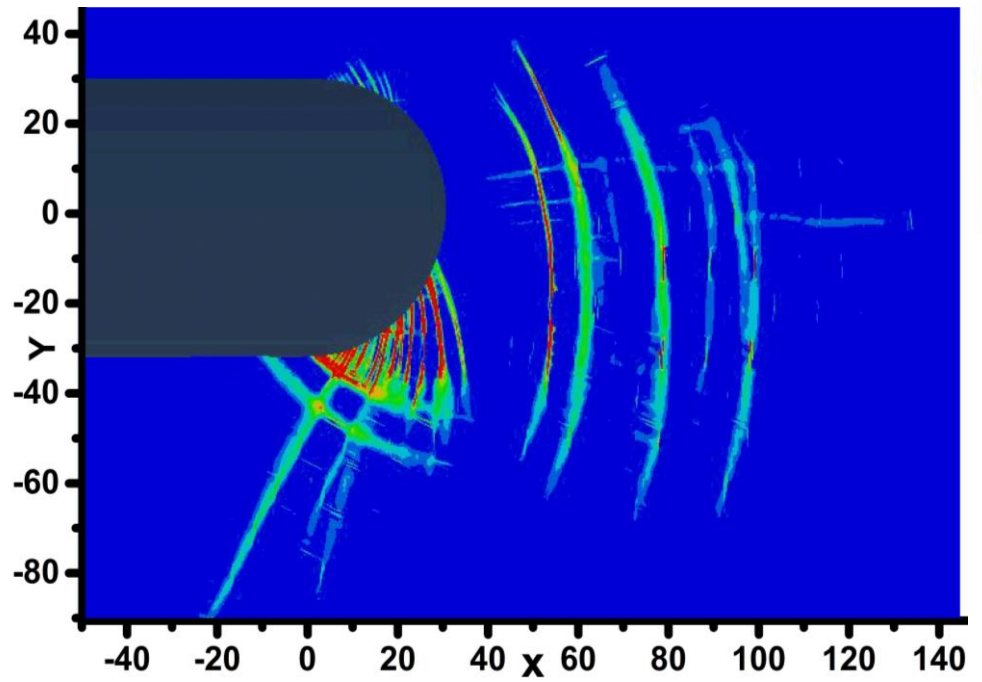


Fig. 8- contour plots of Logarithmic Plastic Strain [$\log \lambda_1^p$] for the corresponding M^e values for the Notch Size [R] = 13 nm and Average Grain Size [d] = 10 nm (on x and y axis in contour plots are distance up to which shear band propagating in nm in respective direction)

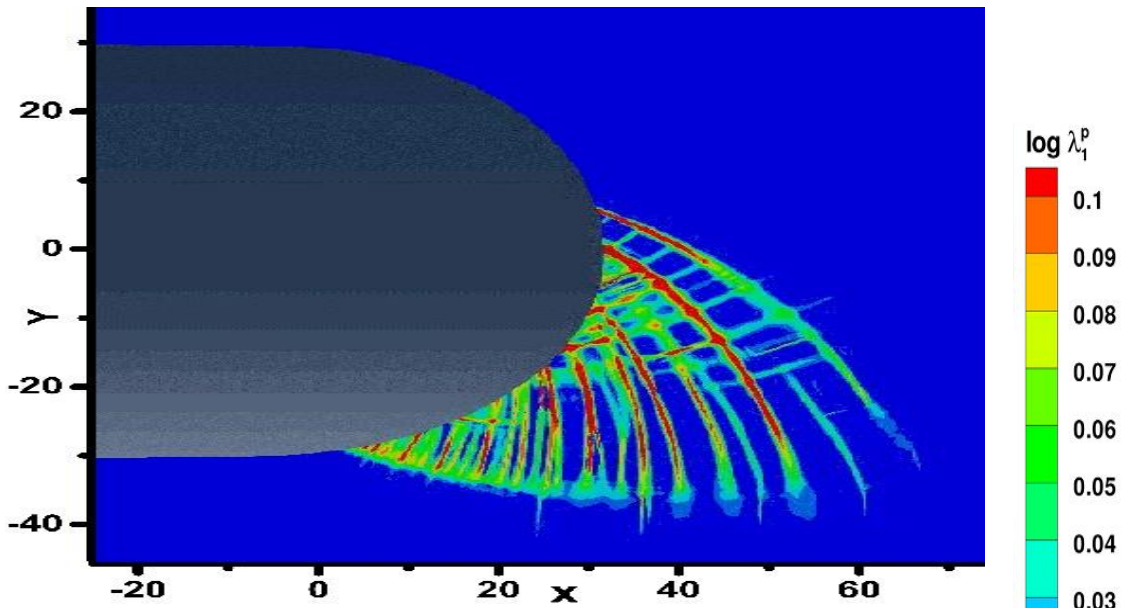
$M^e = 0$



$M^e = 0.25$



$$M^e = 0.75$$



$$M^e = 1$$

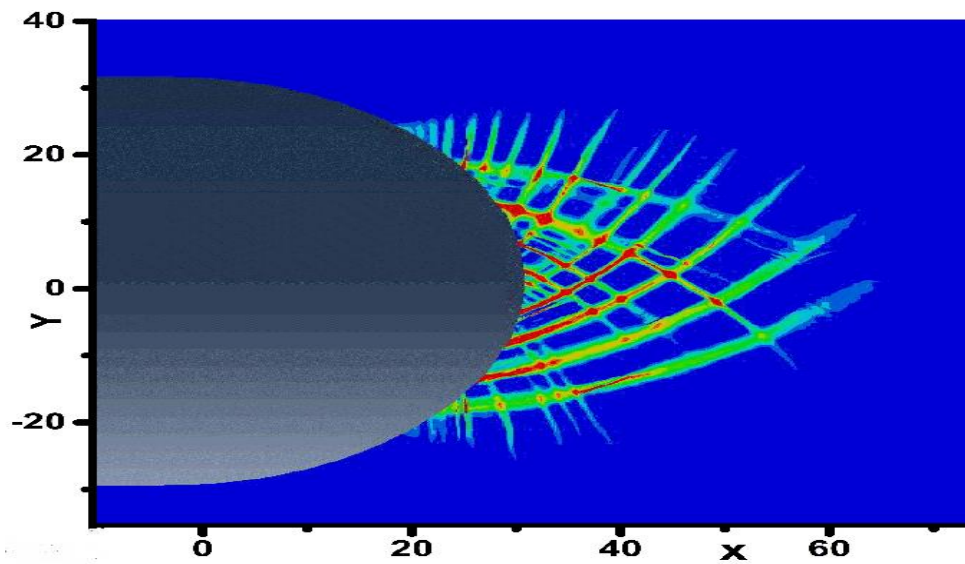
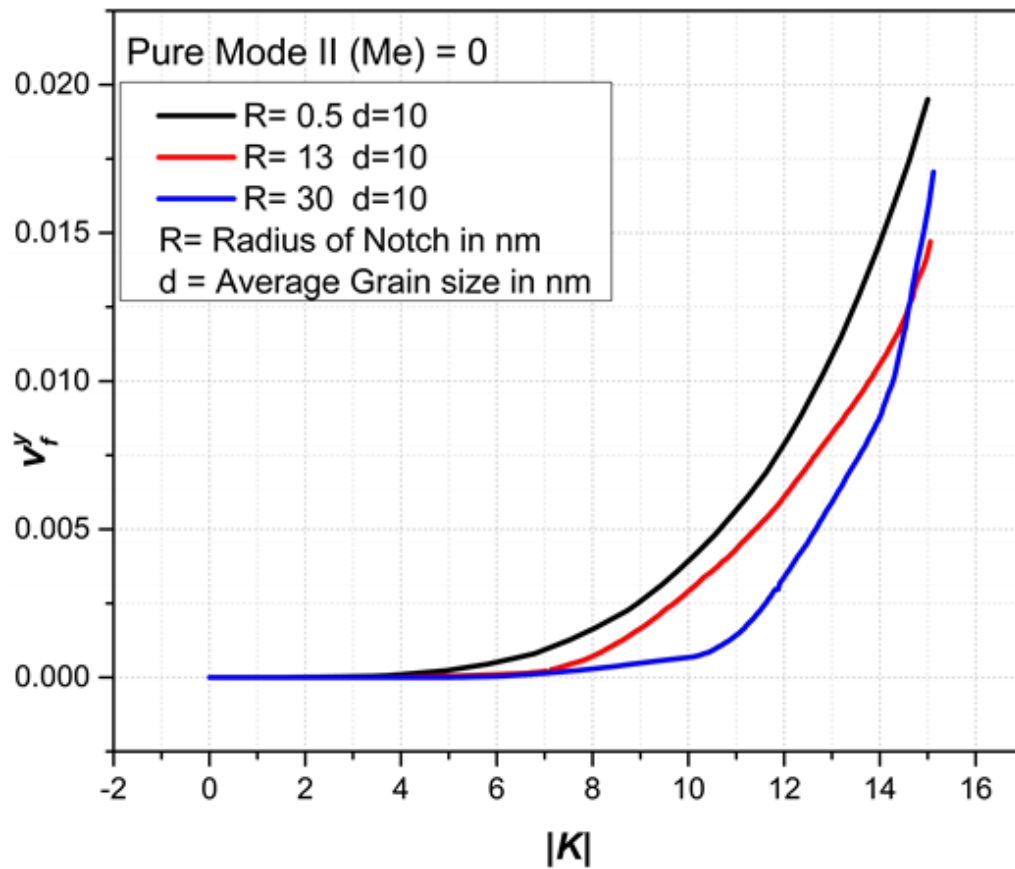


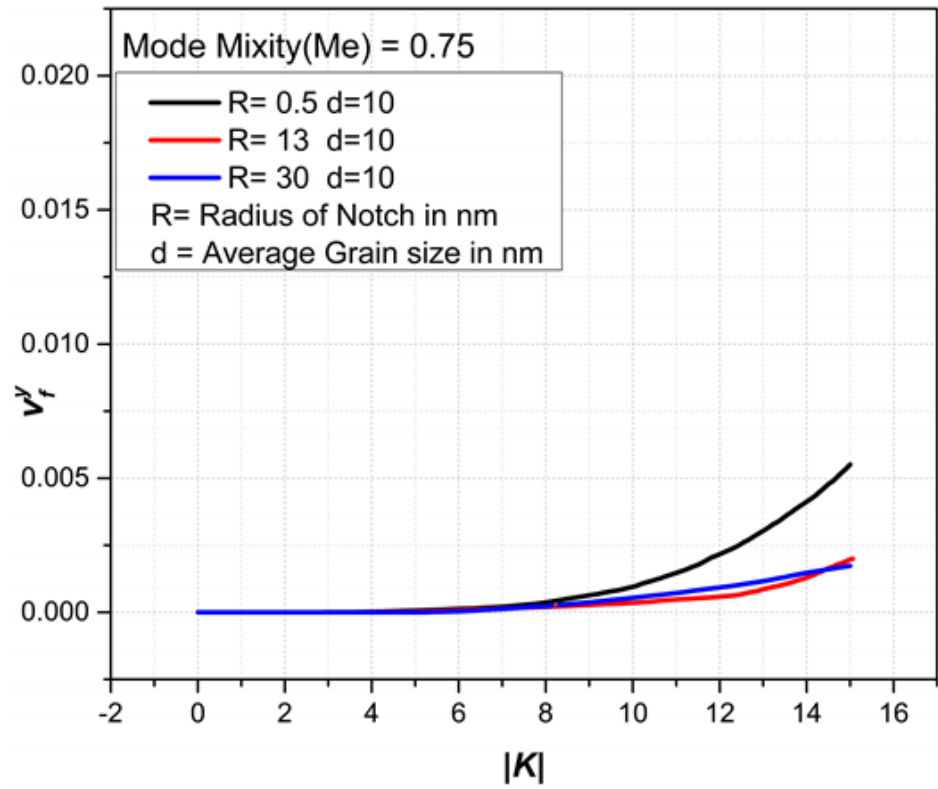
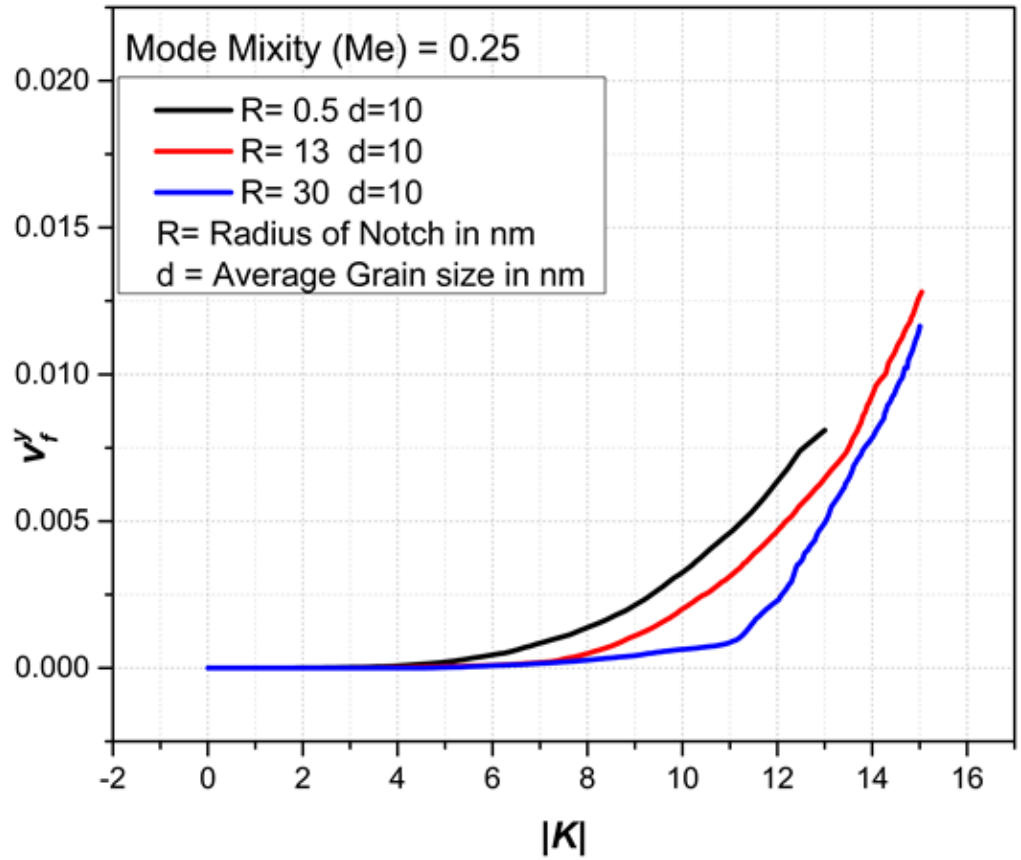
Fig. 9- contour plots of Logarithmic Plastic Strain [$\log \lambda_1^p$] for the corresponding M^e values for the Notch Size [R] = 30 nm and Average Grain Size [d] = 10 nm (on x and y axis in contour plots are distance up to which shear band propagating in nm in respective direction)

The contour plots of the effect of notch size (for the notch radius of 0.5, 13, 30 nm and average grain size of 10 nm) for the M^e values of 0, 0.25, 0.75, 1 is displayed in figures above. All the given contour plots is plotted at rate of loading ($|K|$) 15. Here the horizontal and vertical distance up to which shear band is propagated under the u_x and u_y displacement is shown on the x and y axis. Here the minimum and maximum limit of logarithmic plastic strain is set as 0.001 and 0.1. As the loading rate ($|K|$) is increases so many shear bands are stemming from the notch surface and extending in the radial direction, we can viewed in contour plots. The values of plastic strain are indicated by colour as per their intensity. The length of the shear band is increasing as the loading rate value ($|K|$) increases. . The intensity of plastic strain inside the shear bands is decreasing as shear band is going away from the notch due to the large plastic strain gradient inside shear band. It is easily noticed that for the M^e values of 0, 0.25 ($R= 0.5, 13, 30\text{nm}$) and for $M^e = 0.75, 1$ ($R=0.5 \text{ nm}$) some of the shear bands stemming from the notch in radial direction and these radial shear bands are intersecting almost orthogonally by secondary type of shear bands. The secondary types of shear bands in case of notch radius 0.5nm is propagating through the interfaces but for other cases it is propating through interface as well as grain. The shear bands are propagating upto 180nm in case of $M^e = 0$ whereas it is upto 140 nm for $M^e =0.25$ for notch radius of 0.5, 13nm. The length of lower lobe shear band is increasing beyond -80 nm for $M^e = 0.25$ as compare to $M^e = 0$. The Plastic zone lobe is symmetrically coincide with x axis line ahead of the notch for $M^e = 1$ cases. The clockwise rotation of Plastic zone gets more visible when M^e value is increased to 0.75. For the $M^e = 0.75$ plastic zone lobe is rotates clockwise in lower half plane approximately to $\theta = -30^\circ$ (measured from the centre of the notch or notch tip to node (from which shear band is start to propagate ahead of the notch tip) in the undeformed configuration) but for the both cases $M^e = 1, 0.75$ plastic zone

size in x direction is remains constant up to 60 nm whereas for y direction also it is approximately same. Plastic zone for the M^e values 1, 0.75 is concentrated near the notch only whereas for the M^e values 0, 0.25 it is concentrated near the notch for some amount and scattered in large amount ahead of notch. By observing all images we can say that as the M^e value is increasing the plastic zone size is decreasing.

5.1.2 The effect of M^e on the Evolution of Plastic Zone size in Nanoglass





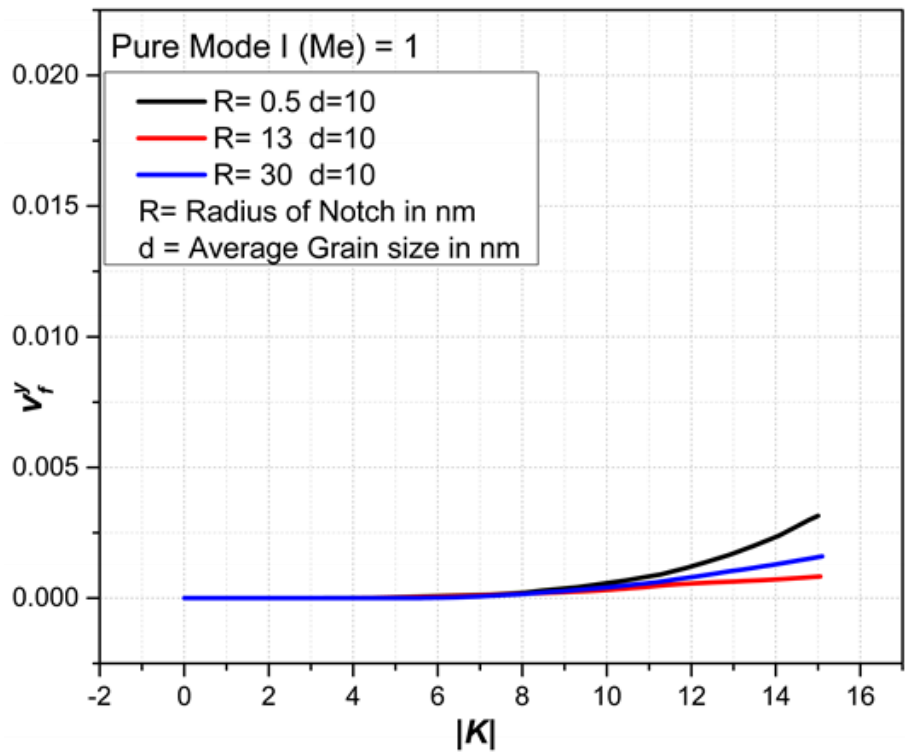
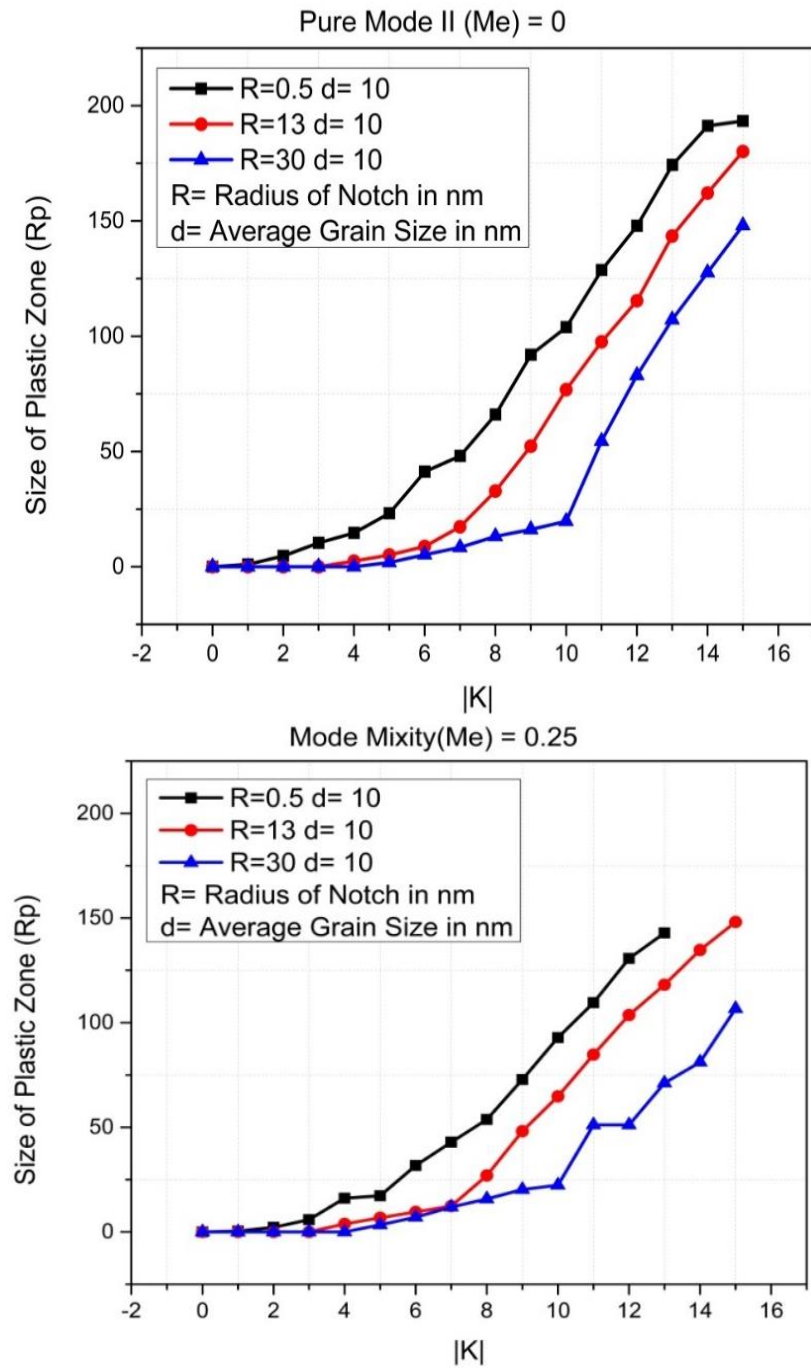


Fig. 10- Variation of volume fraction [v_f^y] of material undergoing in plastic yielding with increase in loading factor for corresponding M^e values

5.1.3 Effect of Mode Mixity on Plastic zone size [maximum length of shear band] in Nanoglass



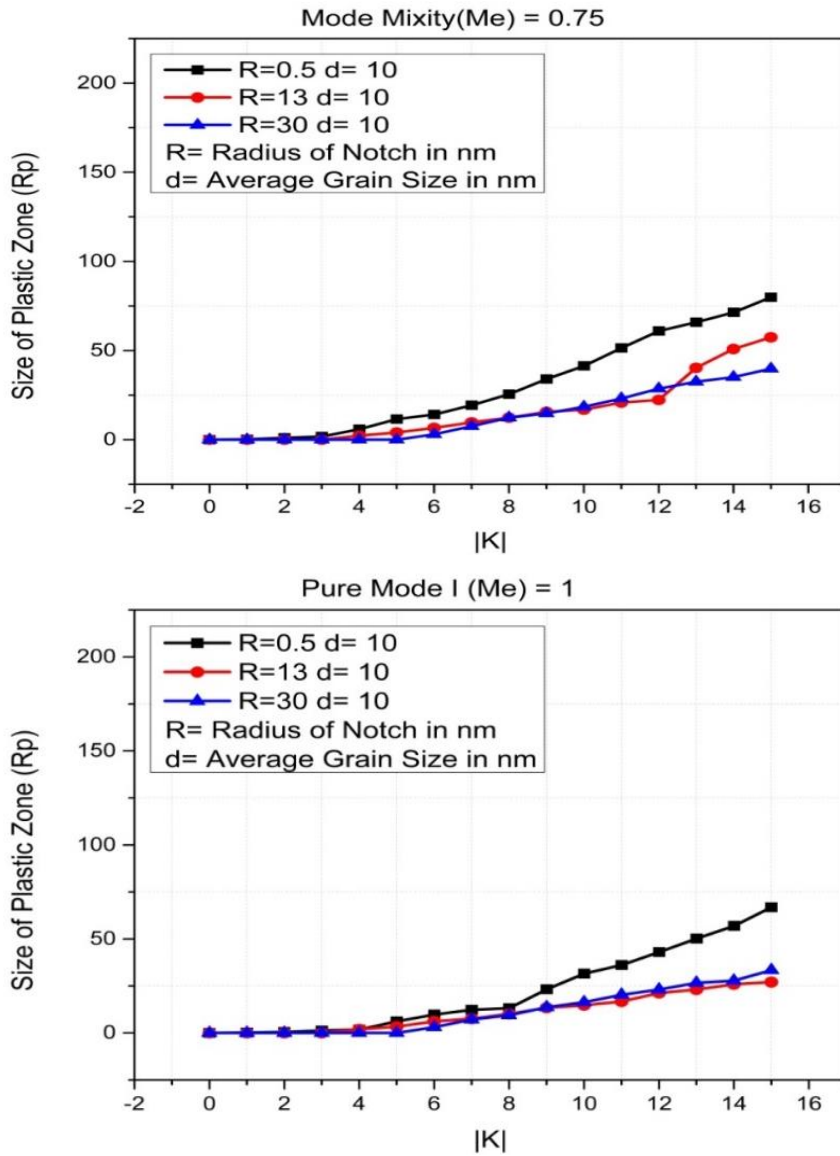


Fig. 11- Variation of Plastic Zone size [maximum length of Shear Band] with increase in loading factor [|K|] for corresponding M^e values and Notch Size [R]= 0.5, 13, 30 nm, Average Grain Size [d] = 10 nm

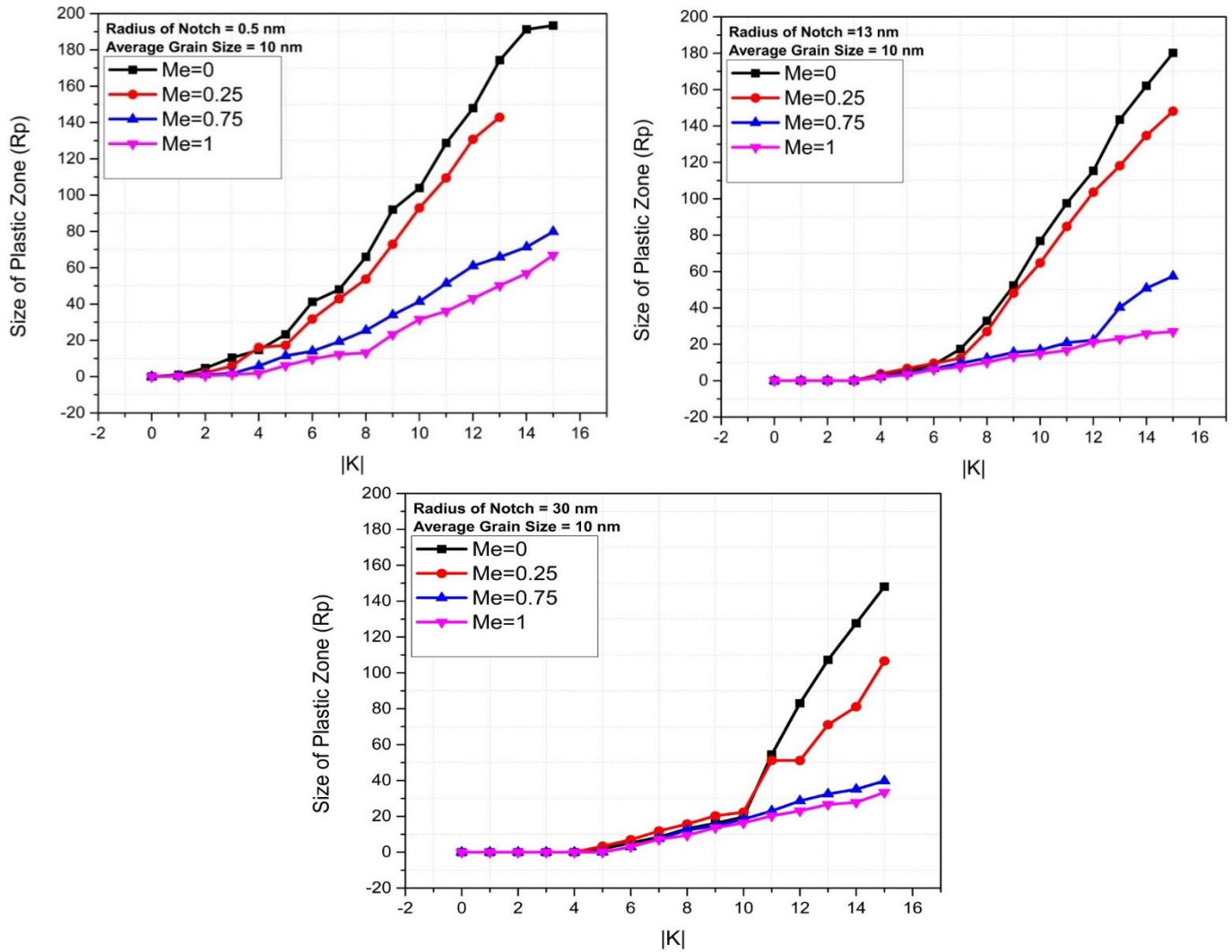


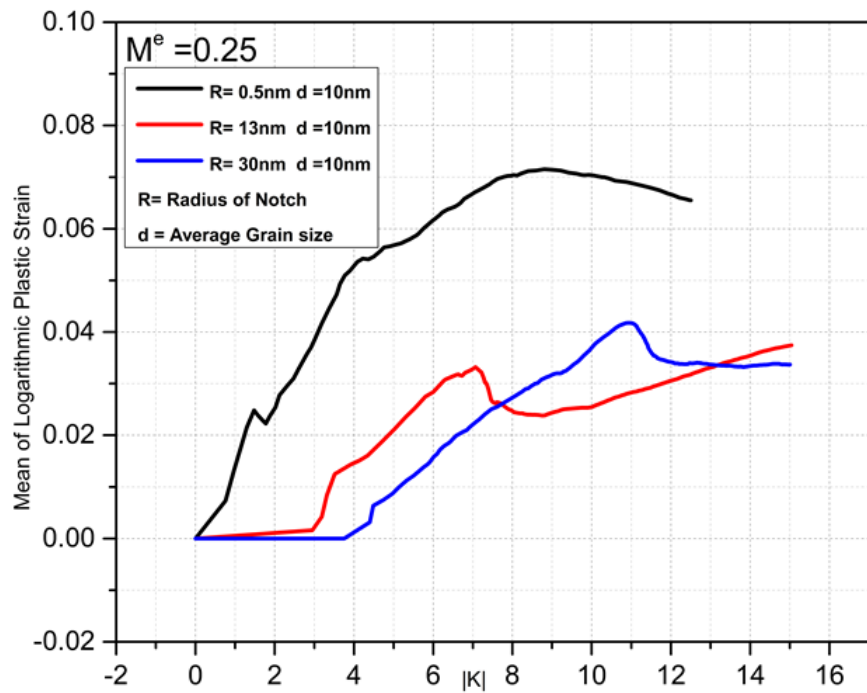
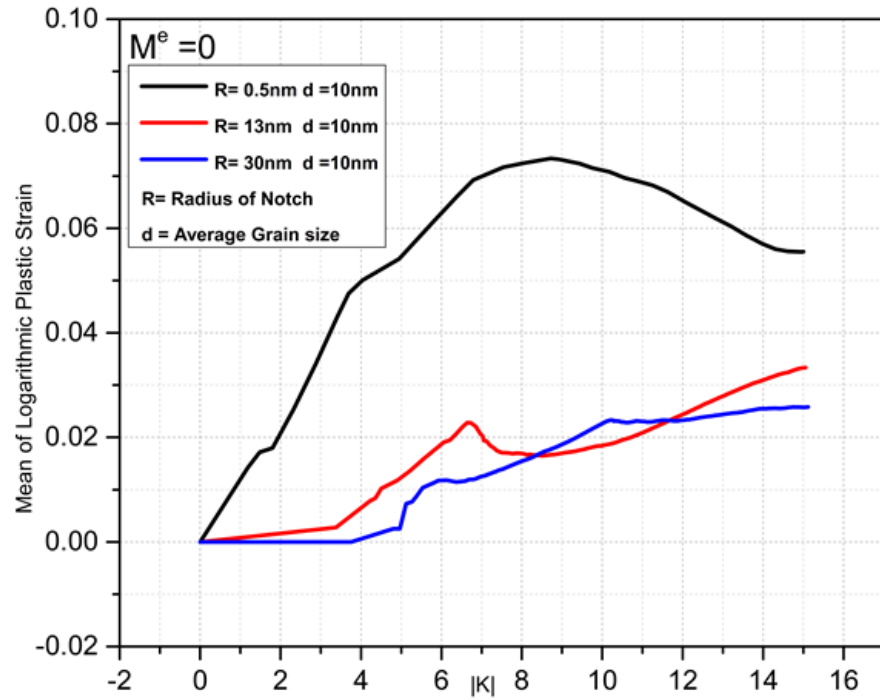
Fig. 12- Variation of Plastic Zone size [maximum length of Shear Band] with increase in loading factor [|K|] for Notch Size [R]= 0.5, 13, 30 nm, Average Grain Size [d] = 10 nm and corresponding M^e values

The volume fraction percentage of material experiencing plastic deformation (V_f^y), is estimated to understand the expansion of the plastic zone ahead of the crack tip as the loading rate progresses. The graphs of Volume Fraction (V_f^y) versus Effective Loading Rate is as shown in above Fig. Plastic yielding in an element is supposed to occur if the greatest

principal logarithmic plastic strain surpasses 0.001 at that point for this purpose. Using this condition, V_f^y for NG are determined and plotted against effective loading rate ($|K|$) for different values of M^e in Fig. respectively. Volume fraction percentage (V_f^y) is almost negligible up to roughly $|K| = 5$, regardless of mode-mixity, but it starts increasing fast for additional increase in $|K|$, indicating significant plastic deformation in NG occurs around $|K| = 5$. By observing all the graphs of volume fraction we can easily noticed that volume fraction is occurs more for the Notch size (R) = 0.5 nm for all the M^e values. For notch size of 13 nm, volume fraction is more as compare to notch size of 30 nm upto $|K| = 14$ for $M^e = 0, 0.25$ and for $M^e = 0.75$ and 1 volume fraction is less upto $|K| = 14$ as compared to notch size of 13 nm. As the M^e value is increasing the volume fraction (V_f^y) is decreasing. As the R/d ratio is increasing the volume fraction (V_f^y) is decreasing for the $M^e = 0, 0.25$. For the same loading rate volume fraction is very high for $R/d \ll 1$, low for $R/d \approx 1$ and neither low nor very high for $R/d \gg 1$ for the $M^e = 0.75, 1$. The graphs of Size of Plastic Zone (R_p) verses Effective loading rate ($|K|$) is as shown in fig. above. The Size of Plastic zone (R_p) is measured as distance of shear band from notch surface to distance upto which it is propagated for each loading rate. By observing all the graphs we can say that As the R/d ratio is increasing Size of Plastic zone (R_p) is also increasing clearly for $M^e = 0, 0.25$. In case of $M^e = 0.75$ Size of Plastic zone (R_p) is remain almost same for notch size of 13 and 30 nm between Effective loading rate of 7 to 11 whereas $M^e = 1$ Size of Plastic zone (R_p) is remain almost same for notch size of 13 and 30 nm between Effective loading rate of 7 to 14. For the same loading rate Plastic zone size is very high for $R/d \ll 1$, low for $R/d \approx 1$ and neither low nor very high for $R/d \gg 1$ for the $M^e = 0.75, 1$. Variation of Plastic Zone size [maximum length of Shear Band] verses increase in loading factor [$|K|$] for Notch Size [R] = 0.5, 13, 30 nm,

Average Grain Size [d] = 10 nm and corresponding M^e values is as shown in fig. above.

5.1.4 Mean and Standard Deviation value of Logarithmic Plastic Strain [$\log \lambda_1^p$]



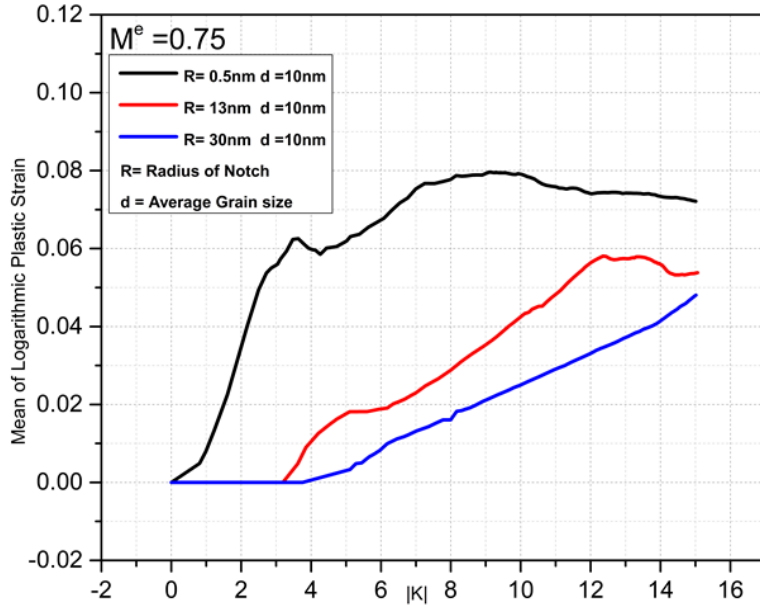
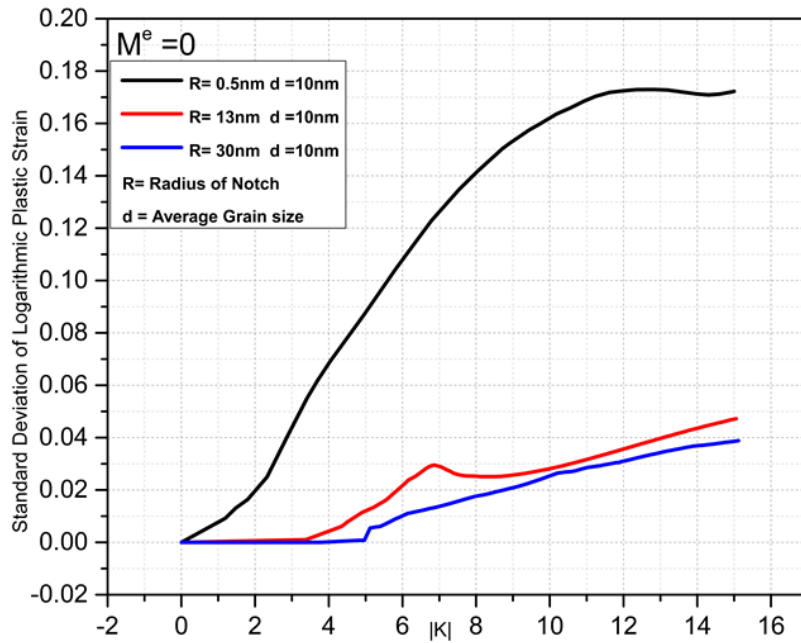
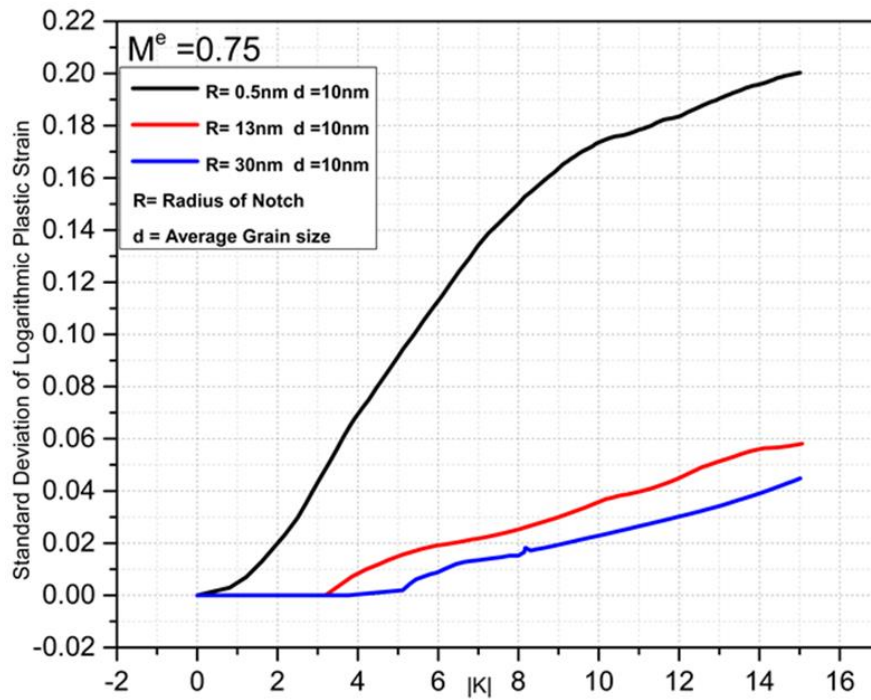
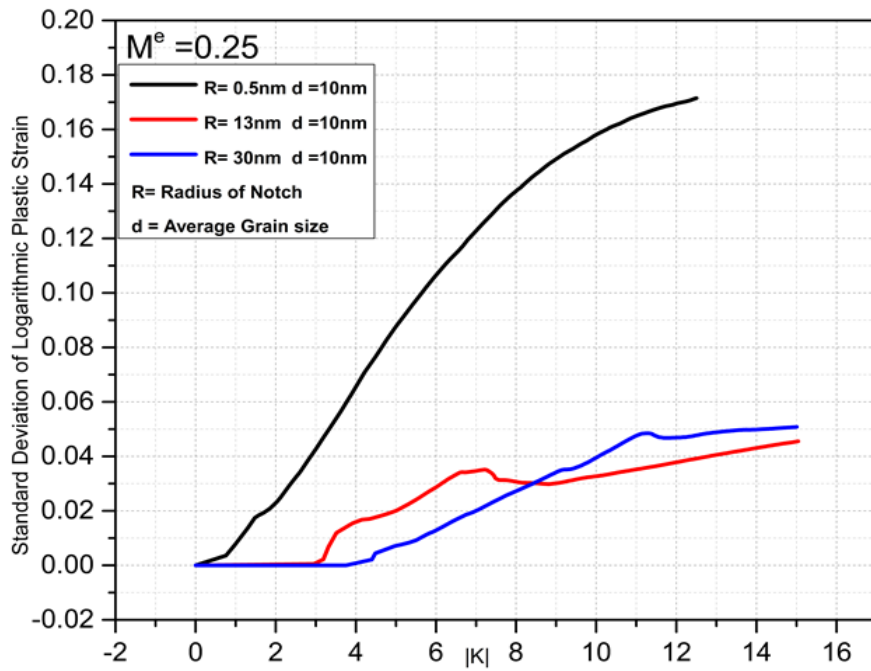


Fig. 13- Variation of Mean value of Logarithmic Plastic strain [$\log \lambda_1^p$] with increase in loading factor [|K|] for Notch Size [R] = 0.5, 13, 30 nm, Average Grain Size [d] = 10 nm and for corresponding M^e values





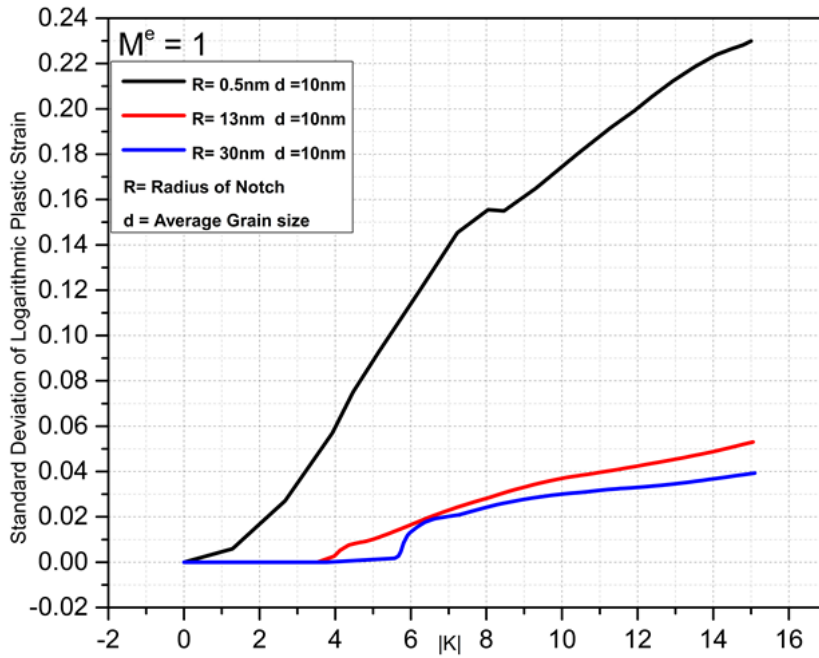
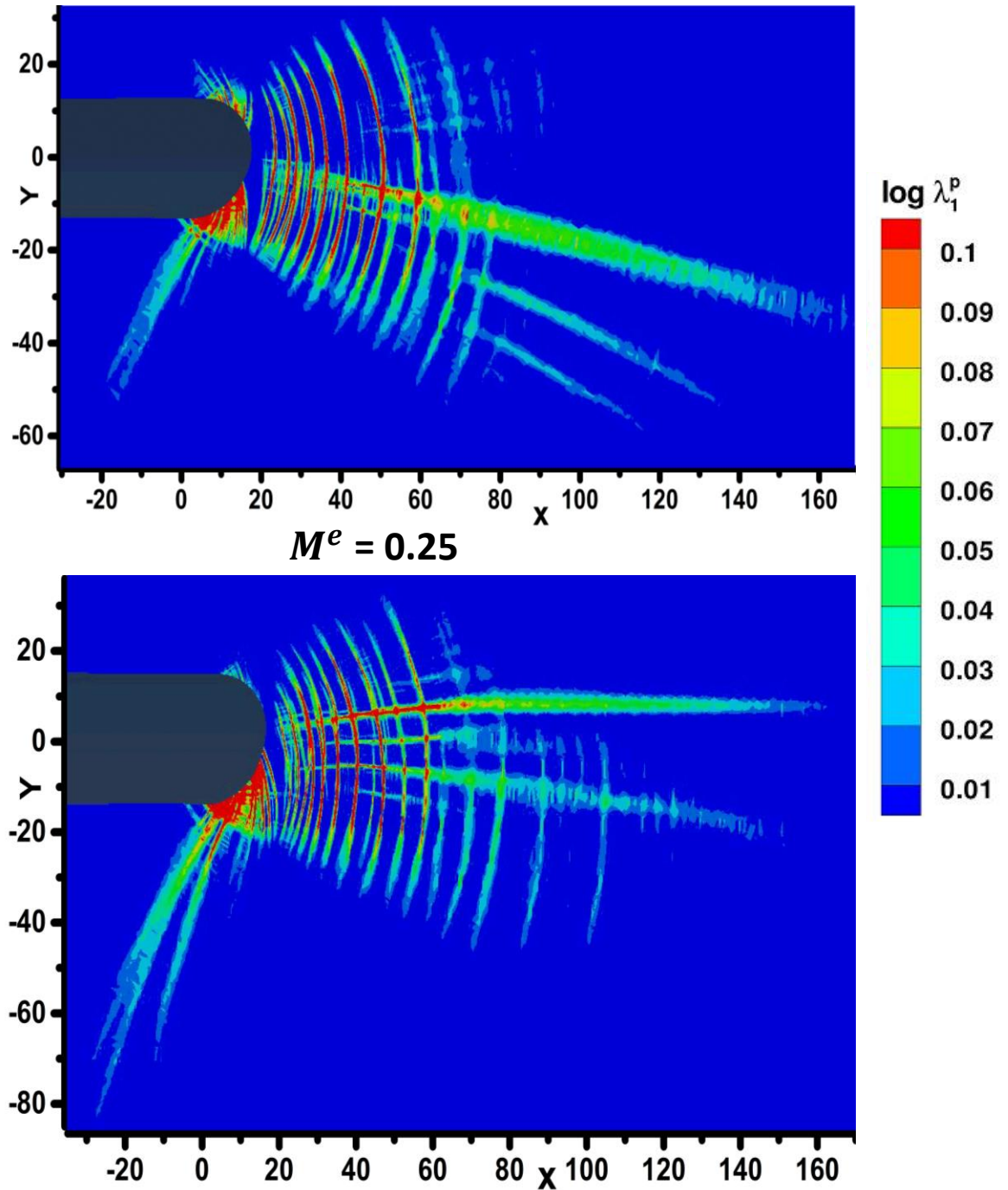


Fig. 14- Variation of Standard Deviation value of Logarithmic Plastic strain [$\log \lambda_1^p$] with increase in loading factor [$|K|$] for Notch Size [R] = 0.5, 13, 30 nm, Average Grain Size [d] = 10 nm and for corresponding M^e values

The graphs of Mean value of Logarithmic Plastic Strain verses Effective loading rate ($|K|$) is as shown in fig. above. In the graph we can clearly observe that mean value of $\log\lambda_1^p$ is very high for Notch Size of 0.5 nm for $M^e = 0, 0.25, 0.75, 1$. For Notch Size of 30, 13 nm Mean value of $\log\lambda_1^p$ is very low and neither low nor very high for $M^e = 0.75, 1$ respectively. The graphs of Standard deviation value of Logarithmic Plastic Strain verses Effective loading rate ($|K|$) is as shown in fig. above. From the graph standard deviation value is high for $R/d \ll 1$, very low for $R/d \gg 1$ and neither low nor very high for $R/d \approx 1$ respectively for $M^e = 0, 0.75, 1$. But in case of $M^e = 0.25$ after Effective loading rate of 8 standard deviation value is getting low for $R/d \gg 1$. If the value of standard deviation is very high or low, it is indicating that pattern of Logarithmic Plastic Strain inside the shear band near or away from notch is heterogeneous or homogeneous respectively.

5.2 Results and discussion for the Effect of Average Grain Size-

5.2.1 Discussion of Contour Plots of Logarithmic Plastic strain



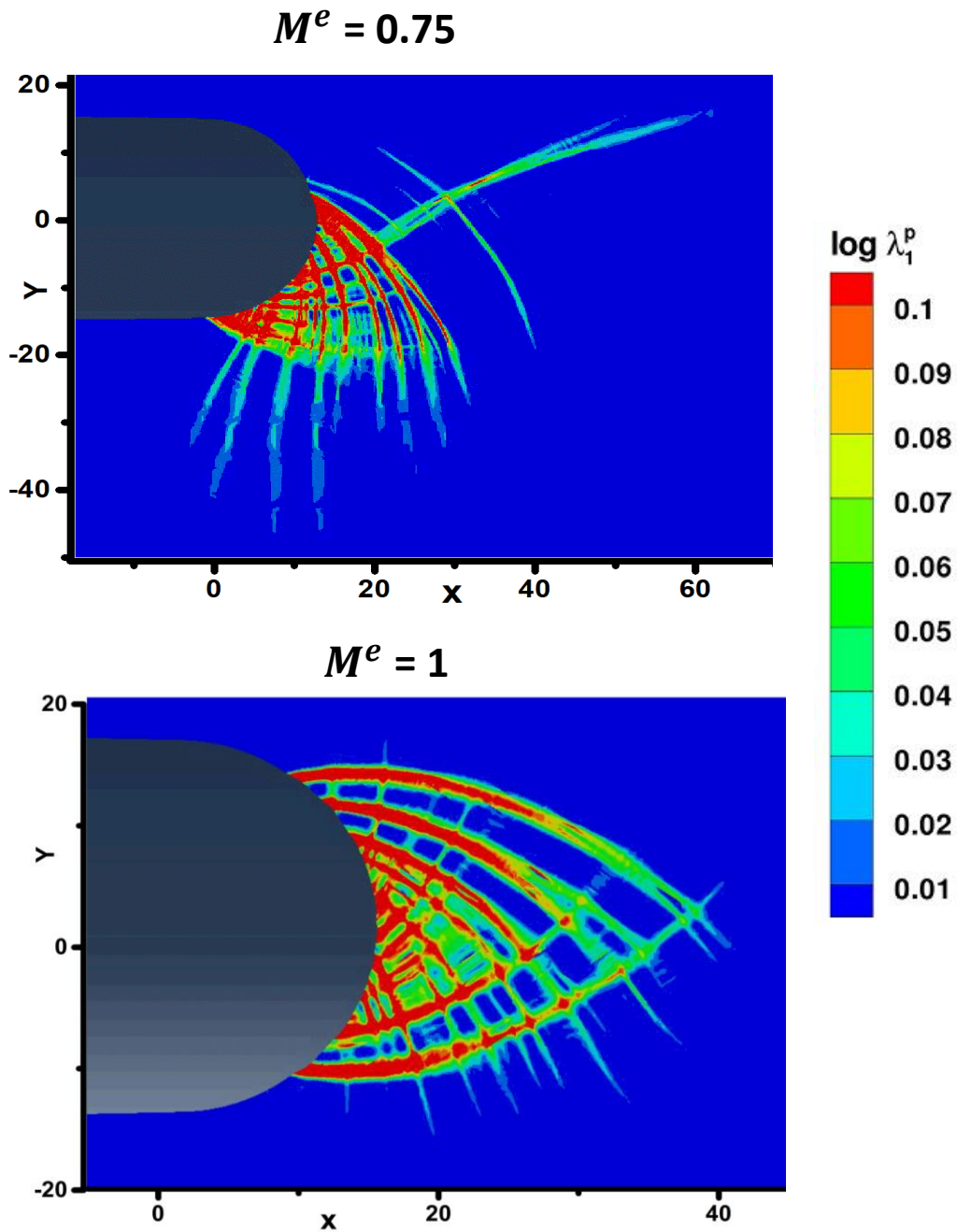
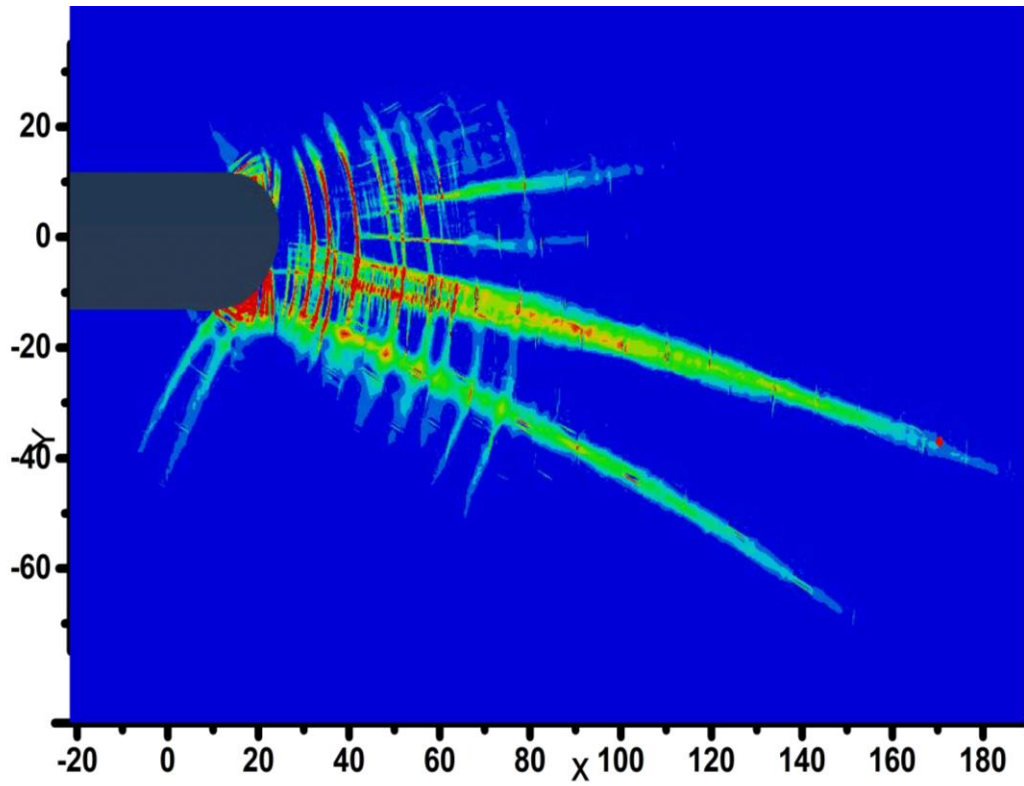
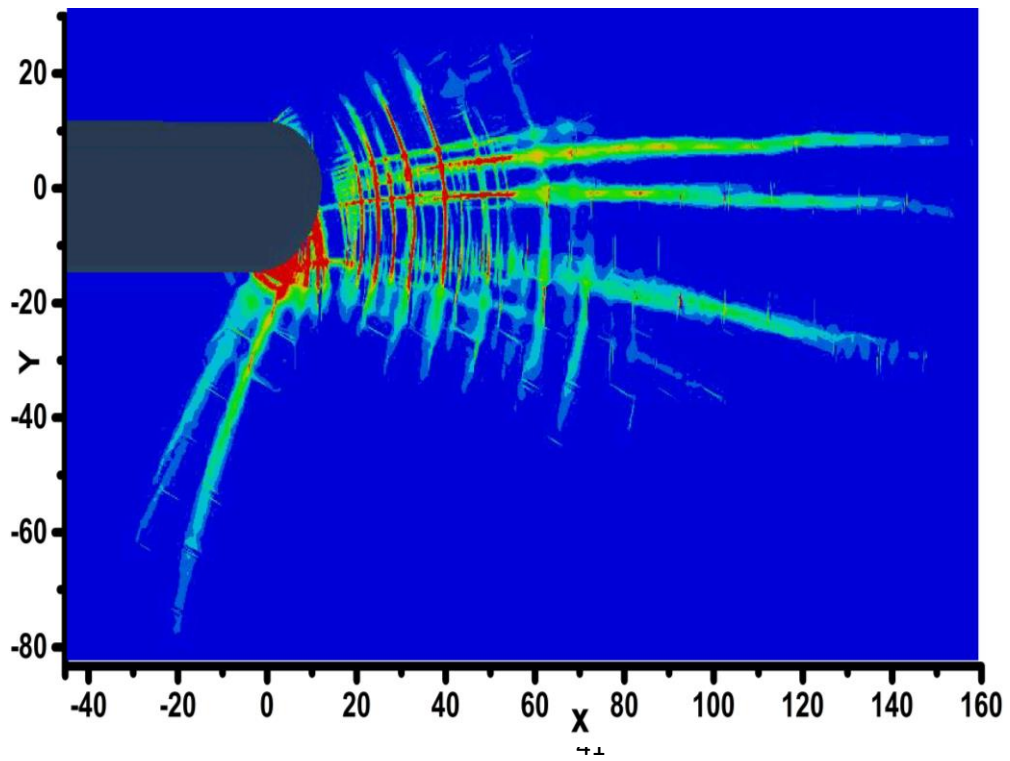


Fig. 15- contour plots of Logarithmic Plastic Strain [$\log \lambda_1^p$] for the corresponding M^e values for the Average Grain Size [d] = 5 nm and Notch Size [R] = 13 nm (on x and y axis in contour plots are distance up to which shear band propagate)

$M^e = 0$



$M^e = 0.25$



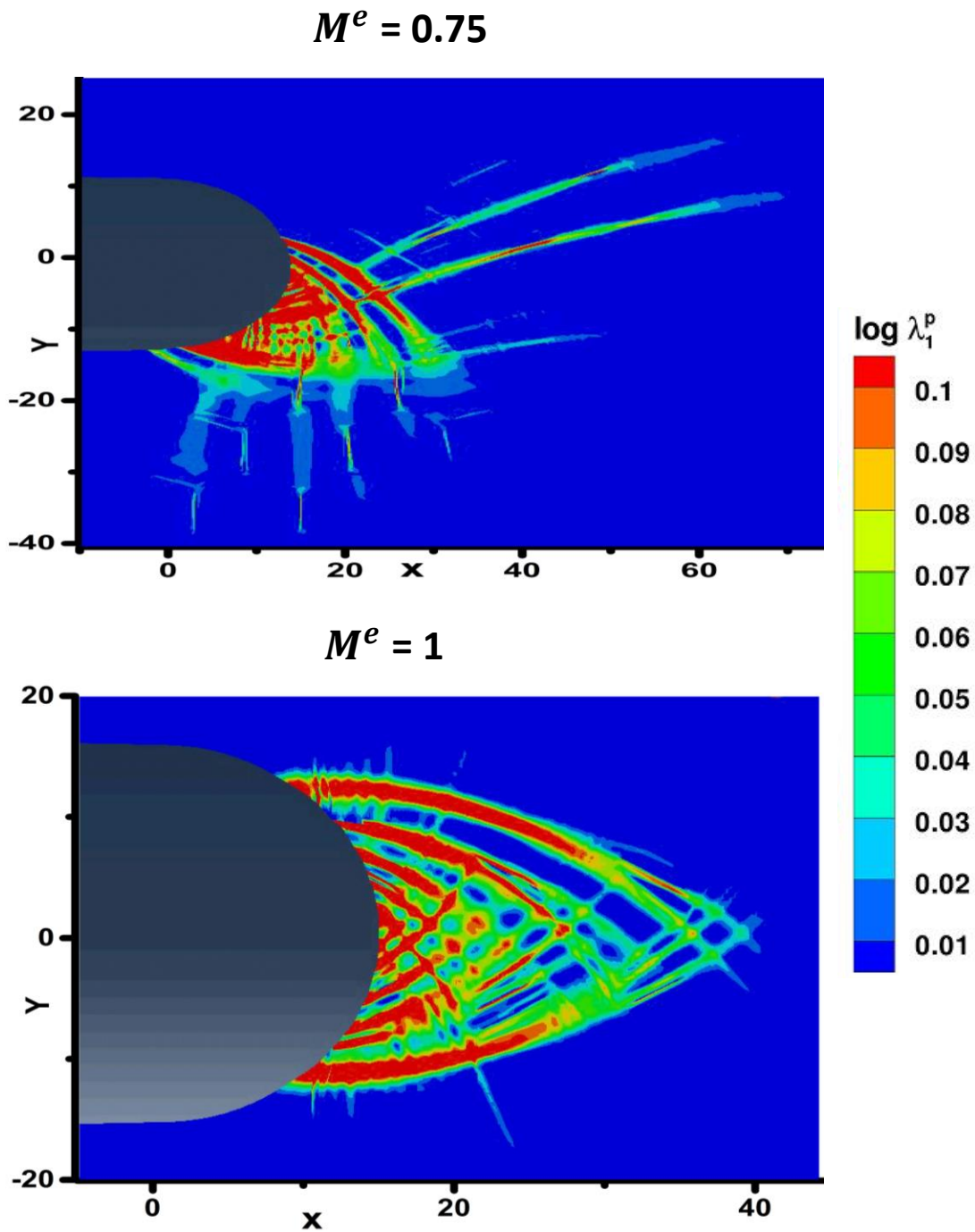
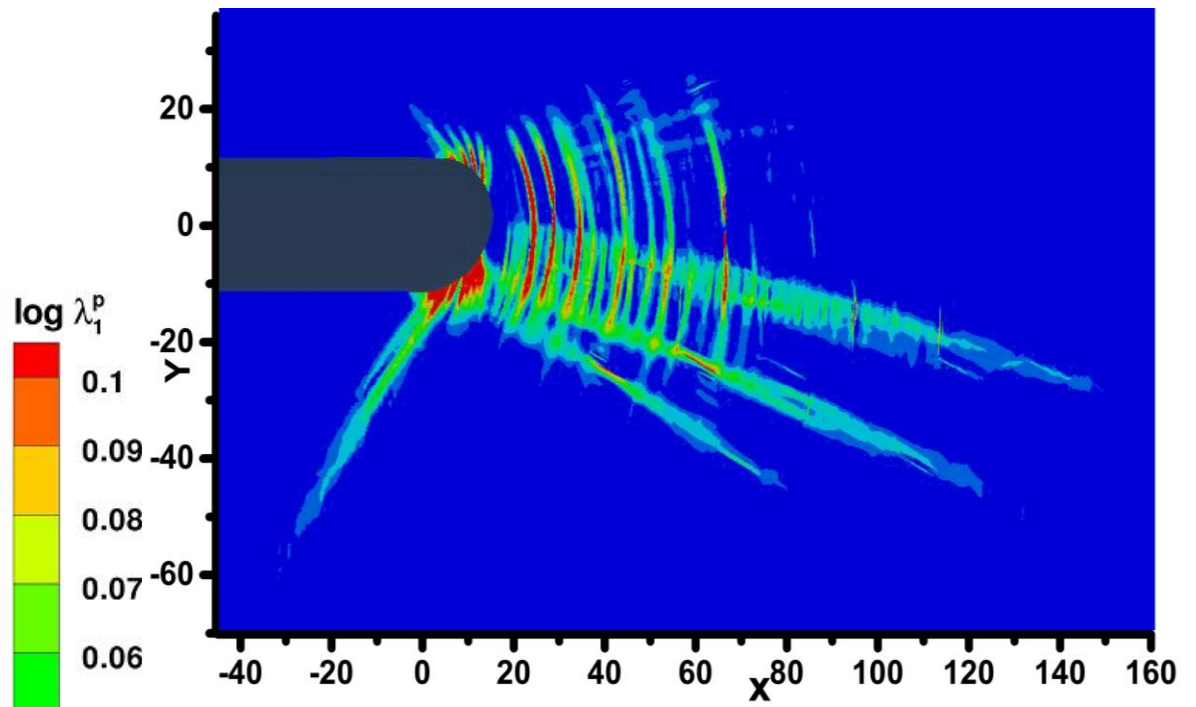
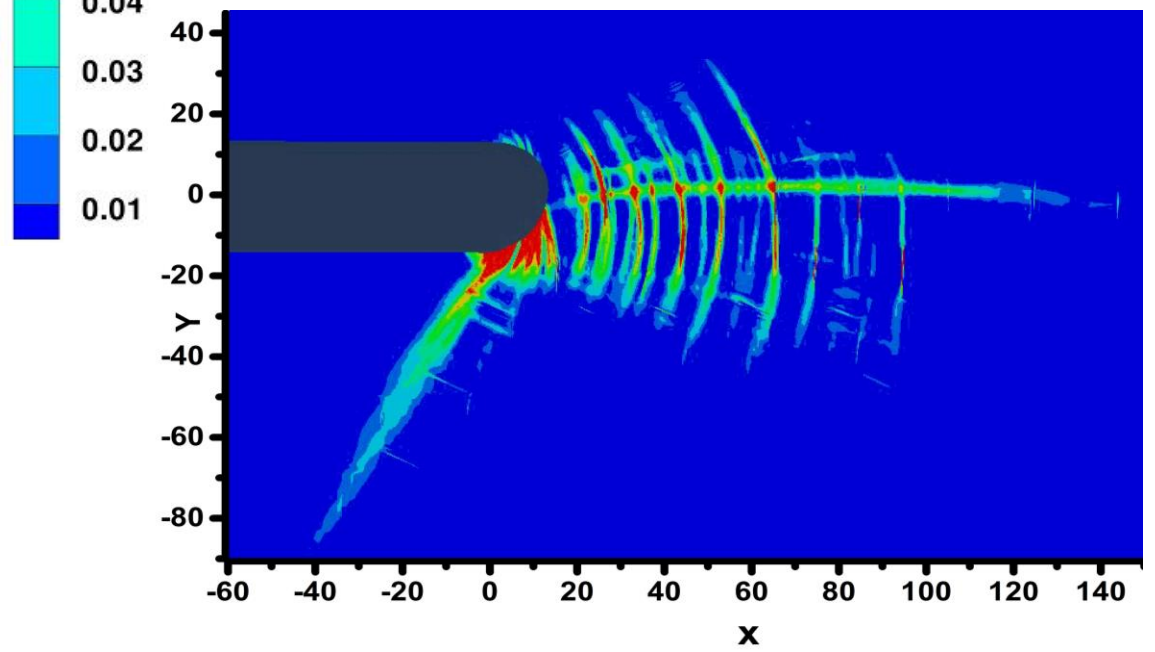


Fig. 16- contour plots of Logarithmic Plastic Strain [$\log \lambda_1^p$] for the corresponding M^e values for the Average Grain Size [d] = 10 nm and Notch Size [R] = 13 nm (on x and y axis in contour plots are distance up to which shear band propagating in nm in respect)

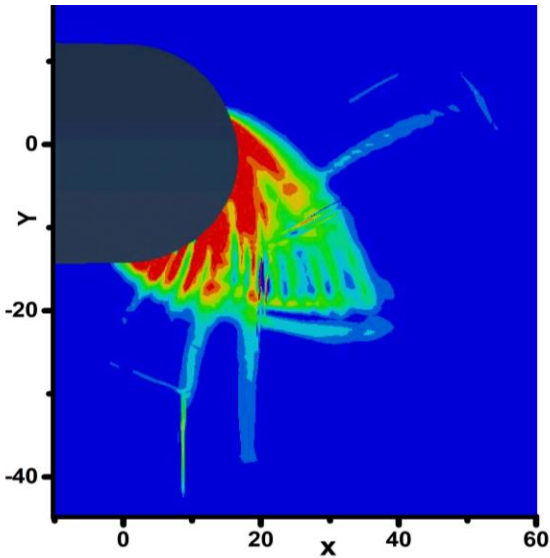
$M^e = 0$



$M^e = 0.25$



$$M^e = 0.75$$



$$M^e = 1$$

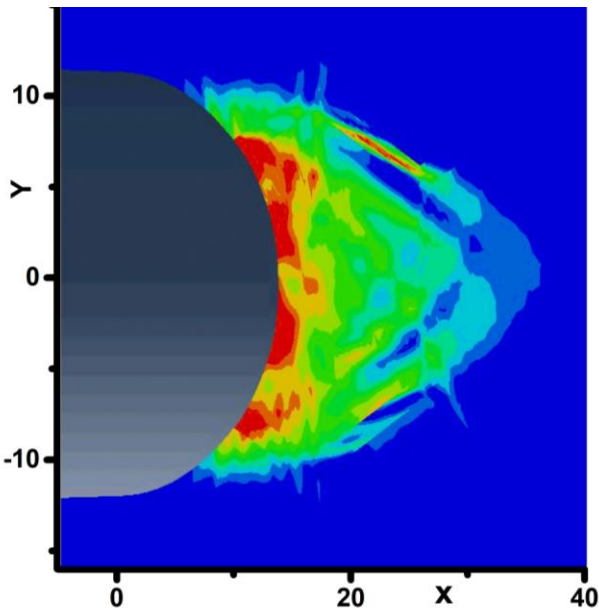
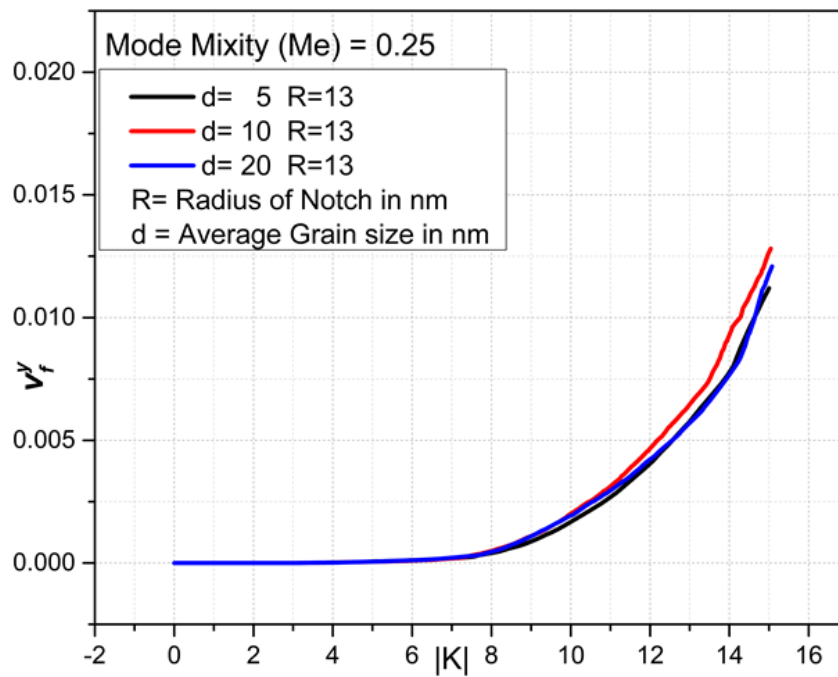
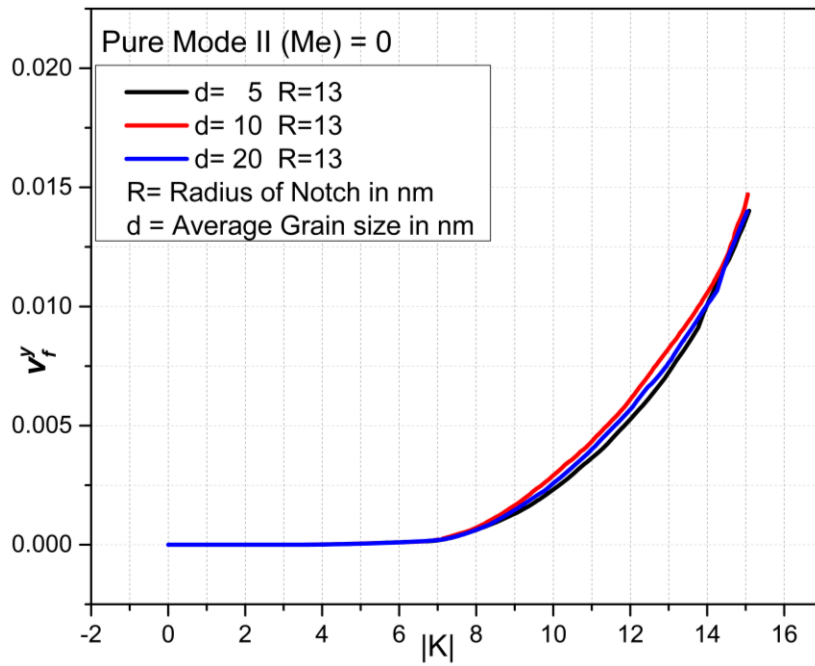


Fig. 17- contour plots of Logarithmic Plastic Strain [$\log \lambda_1^p$] for the corresponding M^e values for the Average Grain Size [d] = 20 nm and Notch Size [R] = 13 nm (on x and y axis in contour plots are distance up to which shear band propagating in nm in respective direction)

The contour plots of the effect of Average grain size (for the average grain size of 5, 10, 20 nm and notch radius 13 nm) for the M^e values of 0, 0.25, 0.75, 1 is displayed in figures above. All the given contour plots is plotted at rate of loading ($|K|$) 15. Here the horizontal and vertical distance up to which shear band is propagated under the u_x and u_y displacement is shown on the x and y axis. Here the minimum and maximum limit of logarithmic plastic strain is set as 0.001 and 0.1. As the loading rate ($|K|$) is increases so many shear bands are stemming from the notch surface and extending in the radial direction, we can viewed in contour plots. The values of plastic strain are indicated by colour as per their intensity. The length of the shear band is increasing as the loading rate value ($|K|$) increases. . The intensity of plastic strain inside the shear bands is decreasing as shear band is going away from the notch due to the large plastic strain gradient inside shear band. It is easily noticed that for the M^e values of 0, 0.25 ($d= 5, 10, 20\text{nm}$) some of the shear bands stemming from the notch in radial direction and these radial shear bands are intersecting almost orthogonally by secondary type of shear bands. The secondary types of shear bands are propagating through the interfaces and grain. The shear bands is propagated upto 160, 140, 60, 40 nm in x direction for the mode mixity values of 0, 0.25, 0.75, 1 for all the cases of effect of grain (As the M^e value is increasing the plastic zone size is decreasing). The length of lower lobe shear band is also increasing as M^e value is increasing upto 0.25. The rotation of Plastic zone gets more visible when M^e value is increased to 0.75. Plastic zone for the M^e values 1, 0.75 is concentrated near the notch only whereas for the M^e values 0, 0.25 it is concentrated near the notch for some amount and scattered in large amount ahead of notch. The Plastic zone lobe is symmetrically coincide with x axis line ahead of the notch tip for $M^e = 1$ cases.

5.2.2 The effect of M^e on the Evolution of Plastic Zone size in Nanoglass



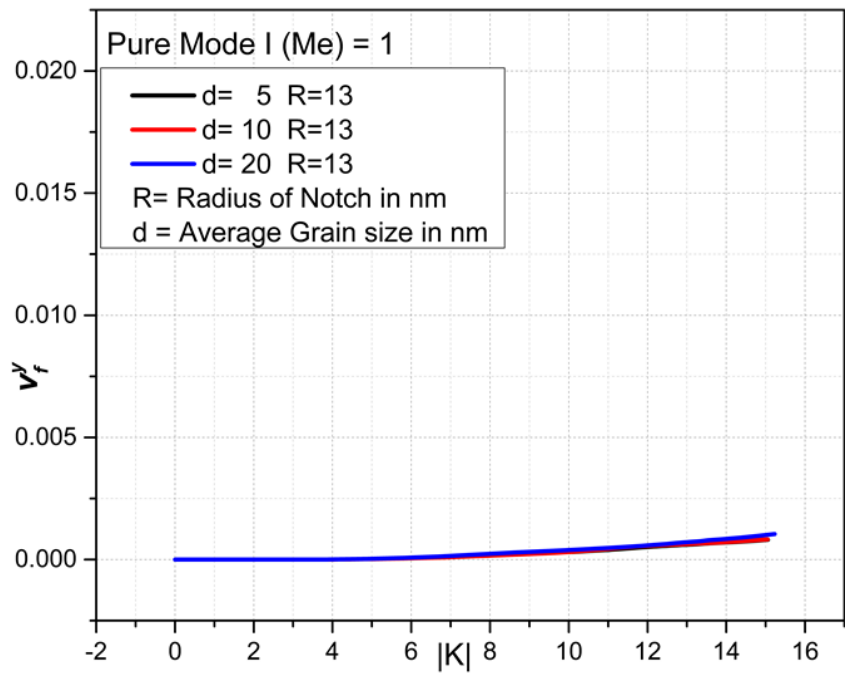
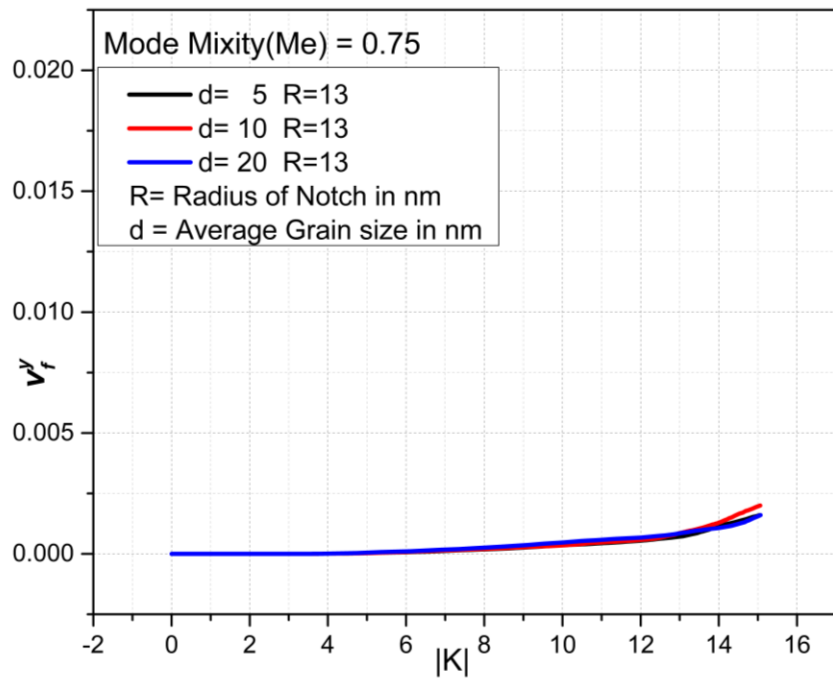
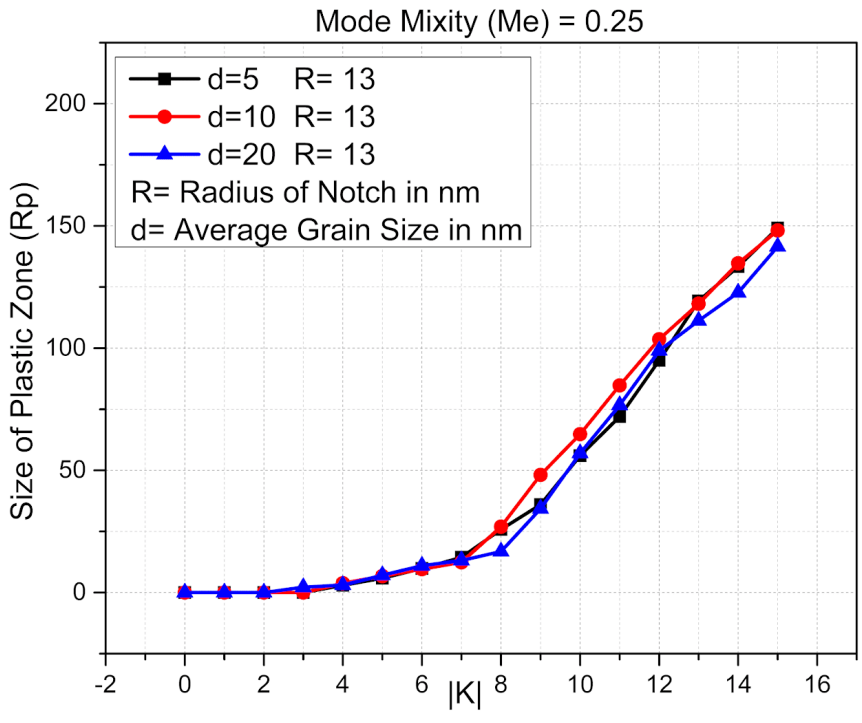
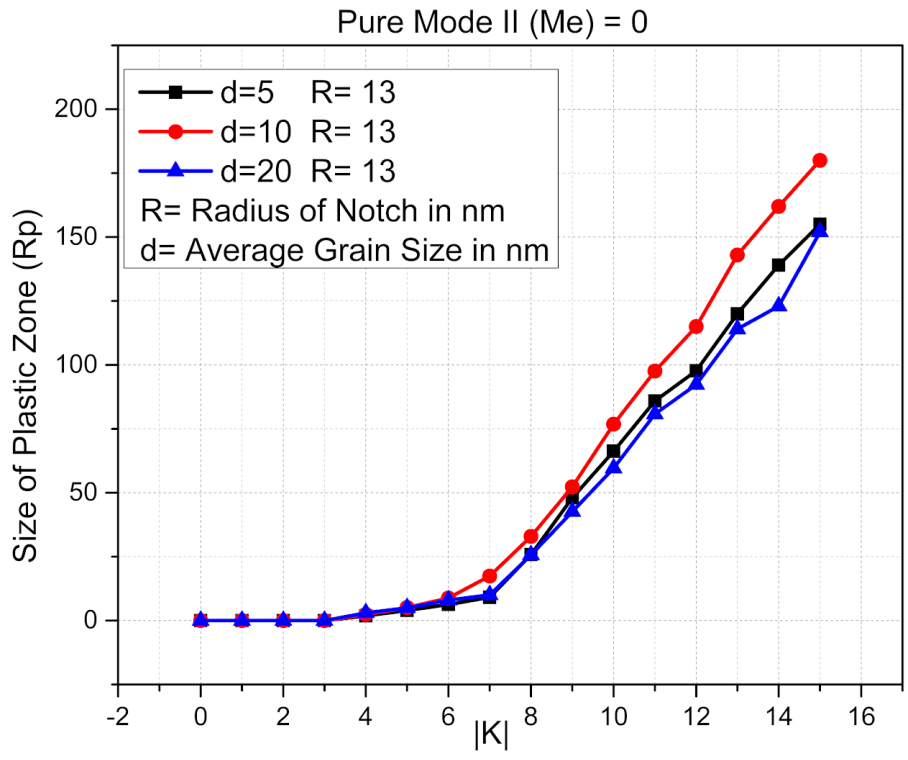


Fig. 18- Variation of volume fraction [v_f^y] of material undergoing in plastic yielding with increase in loading factor for corresponding M^e value

5.2.3 Effect of Mode Mixity on Plastic zone size [maximum length of shear band] in Nanoglass



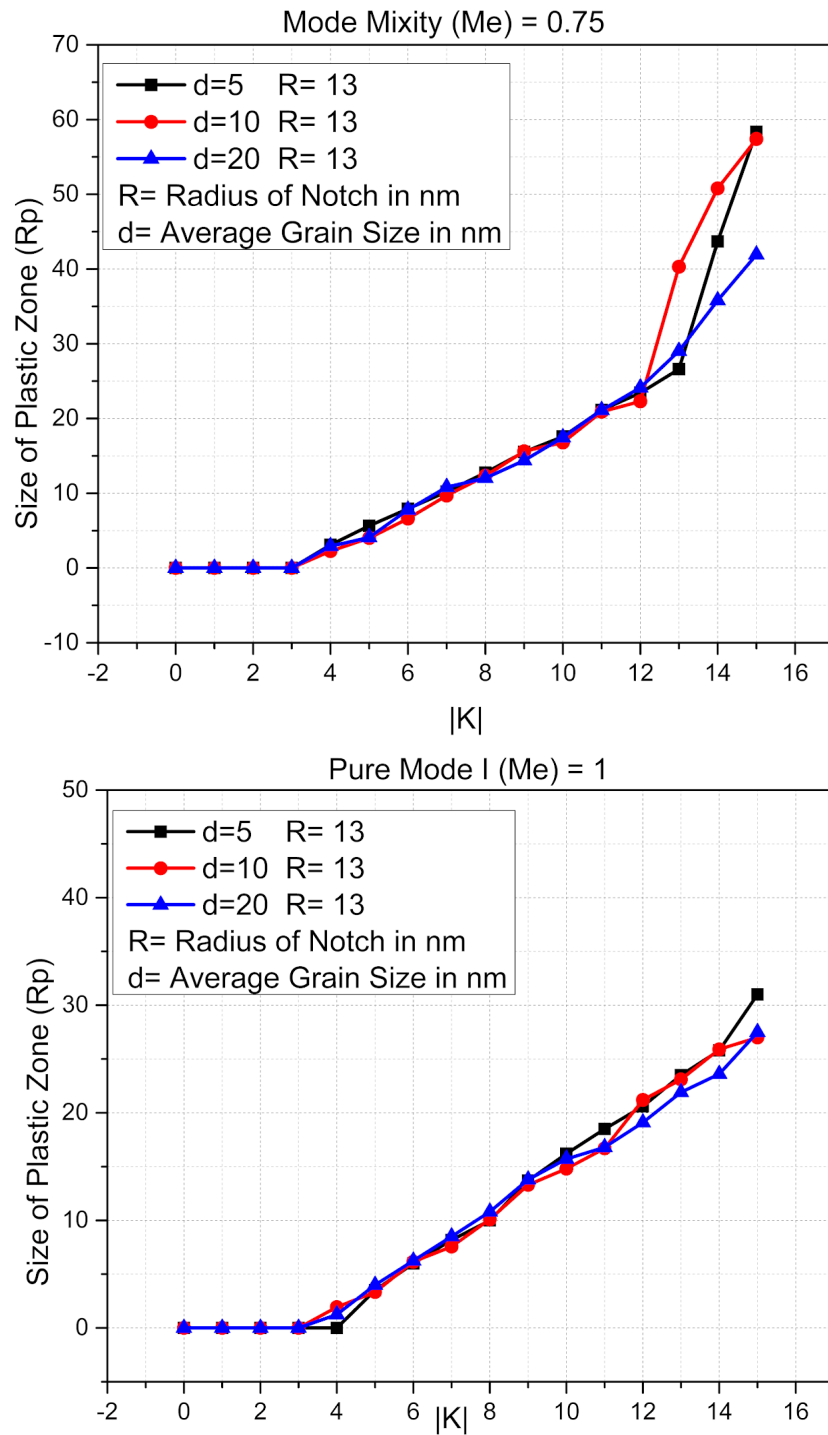


Fig. 19- Variation of Plastic Zone size [maximum length of Shear Band] with increase in loading factor [$|K|$] for corresponding M^e values and Average Grain Size [d] = 5, 10, 20 nm, Notch Size [R]= 13 nm

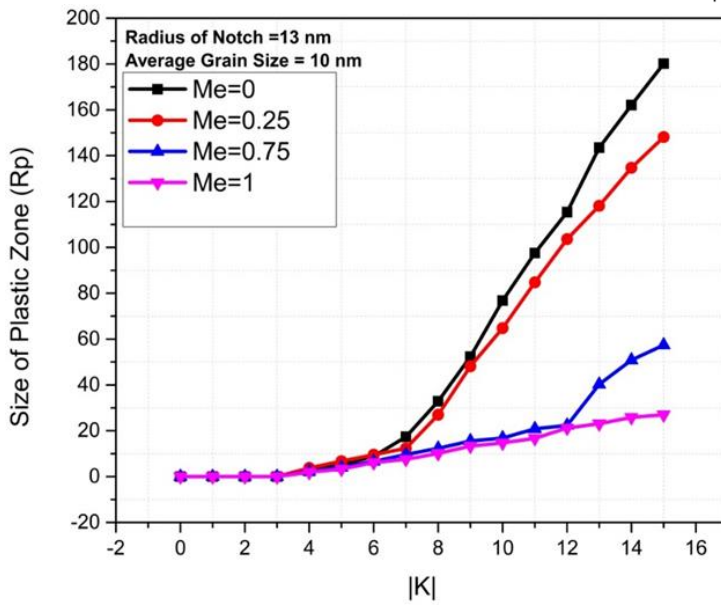
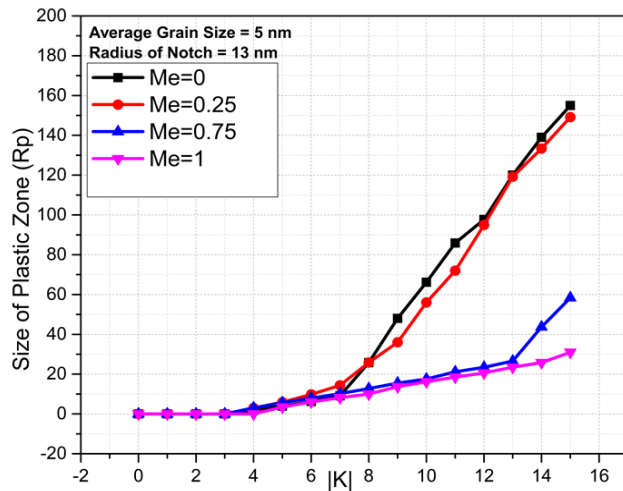
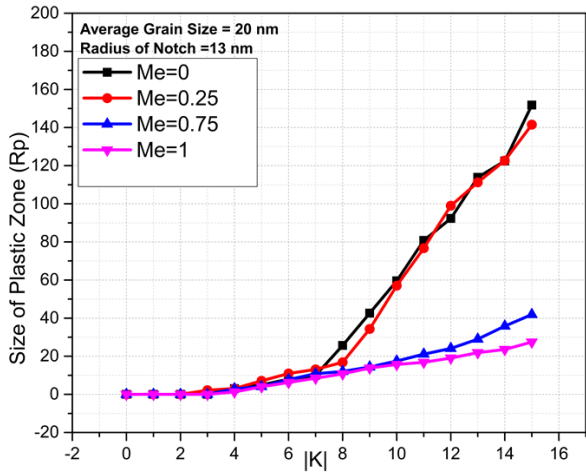


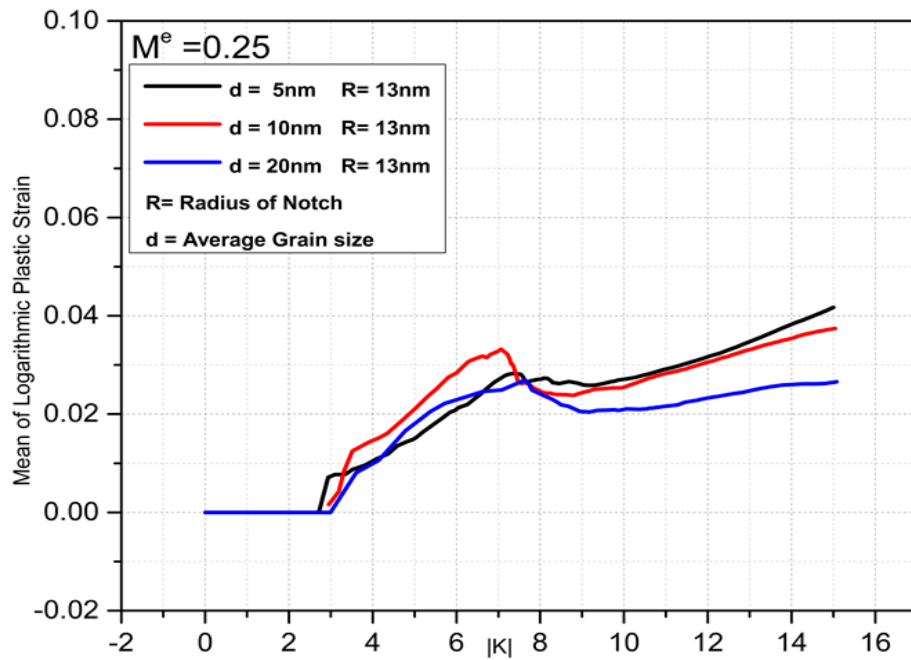
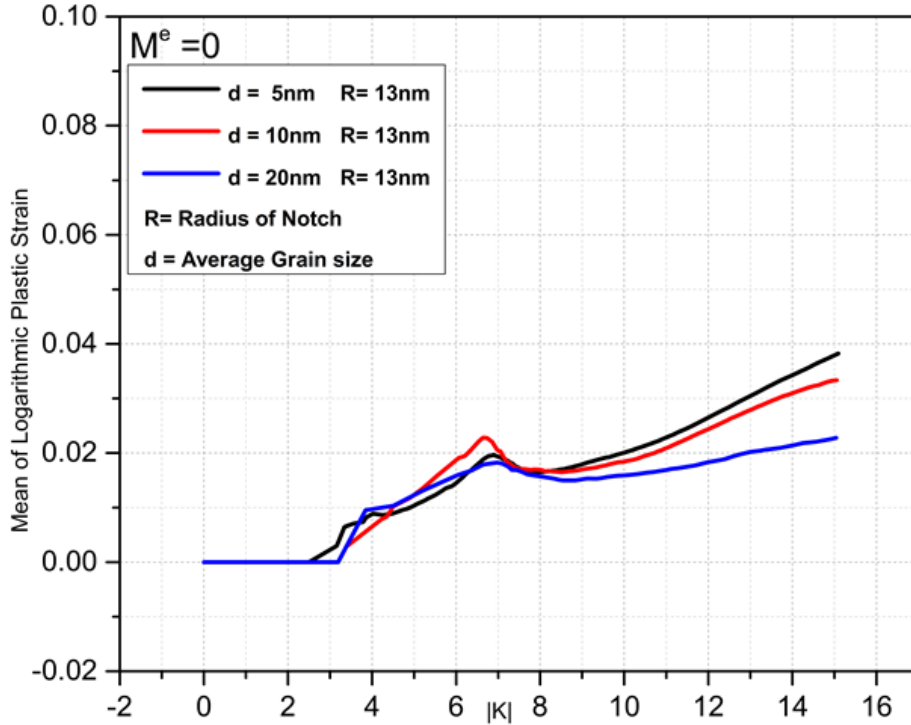
Fig. 20- Variation of Plastic Zone size [maximum length of Shear Band] with increase in loading factor [$|K|$] for corresponding M^e values and Average Grain Size [d] = 5, 10, 20 nm, Notch Size [R]= 13 nm

The volume fraction percentage of material experiencing plastic deformation (V_f^y), is estimated to understand the expansion of the plastic zone ahead of the crack tip as the loading rate progresses. The graphs of Volume Fraction (V_f^y) versus Effective Loading Rate is as shown in above Fig. Plastic yielding in an element is supposed to occur if the greatest principal logarithmic plastic strain surpasses 0.001 at that point for this purpose. Using this condition, V_f^y for NG are determined and plotted against effective loading rate ($|K|$) for different values of M^e in Fig. respectively. Volume fraction percentage (V_f^y) is almost negligible up to roughly $|K| = 7$, regardless of mode-mixity, but it starts increasing fast for additional increase in $|K|$, indicating significant plastic deformation in NG occurs around $|K| = 7$. By observing all the graphs of volume fraction we can easily noticed that volume fraction is occurs more for the Average Grain size (d) = 10 nm and occurs very low for the Average Grain size (d) = 20 nm for the $M^e = 0, 0.25$. Here also we can see same trend, as the M^e value is increasing the volume fraction is decreasing. In case of effect of grain volume fraction is almost remains same, as R/d ratio does not affecting on plastic yielding. The graphs of Size of Plastic Zone (R_p) versus Effective loading rate ($|K|$) is as shown in fig. above. The Size of Plastic zone (R_p) is measured as distance of shear band from notch surface to distance upto which it is propagated for each loading rate. By observing all the graphs we can say that, in case of $M^e = 0, 0.25$ Plastic zone size is high for $R/d \approx 1$, low for $R/d \gg 1$ and neither low nor very high for $R/d \ll 1$. In case of $M^e = 0.75$ Size of Plastic zone (R_p) is remain almost same in between Effective loading rate of 0 to 12 whereas $M^e = 1$ Size of Plastic zone (R_p) is remain almost same in between Effective loading rate of 0 to 10. Variation of Plastic Zone size [maximum length of Shear Band] verses increase in loading factor [$|K|$] for corresponding M^e values and Average

Grain Size [d] = 5, 10, 20 nm, Notch Size [R]= 13 nm is as shown in Fig. above.

5.2.4 Mean and Standard Deviation value of Logarithmic

Plastic Strain [$\log \lambda_1^p$]



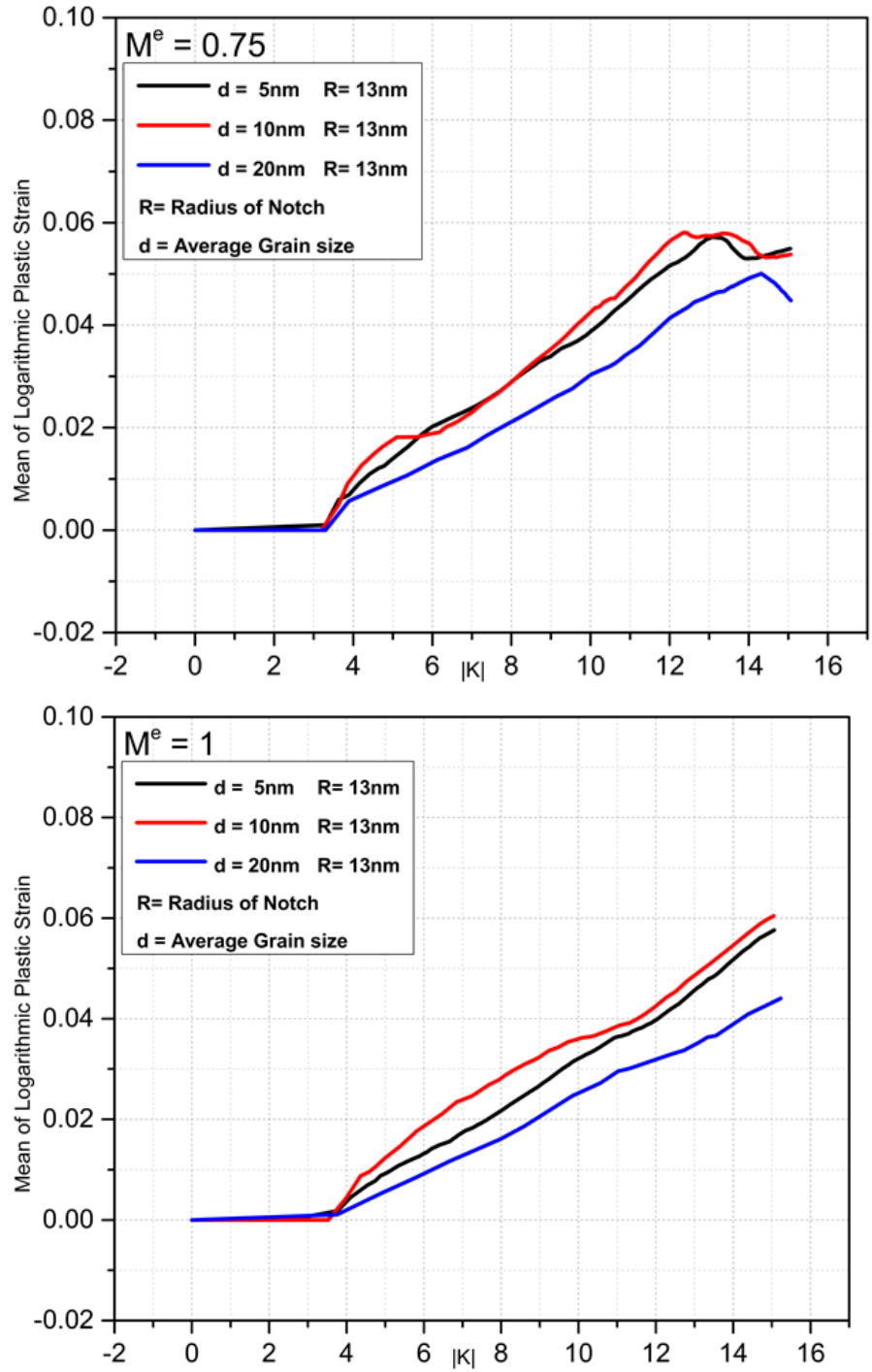
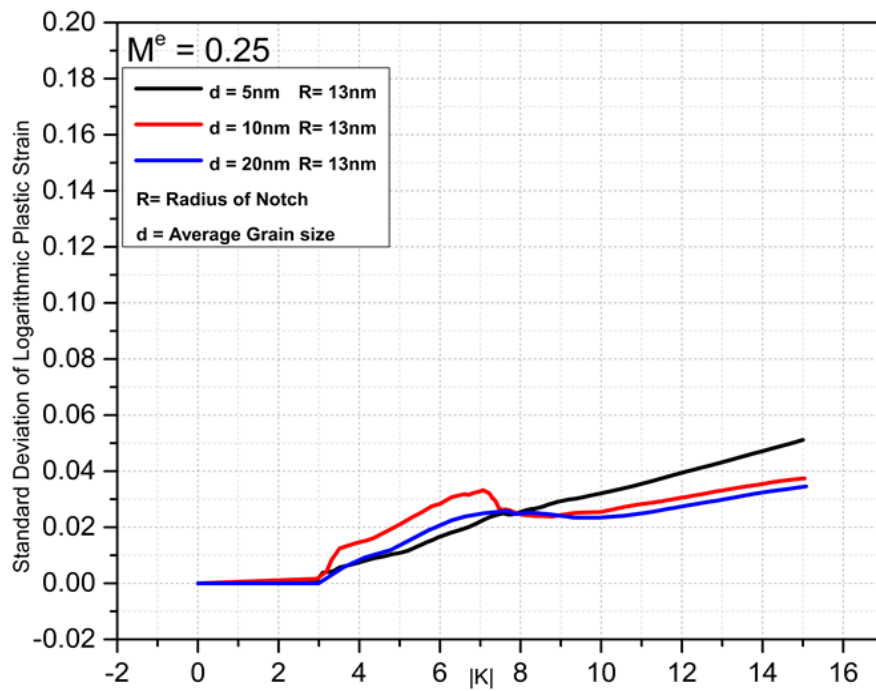
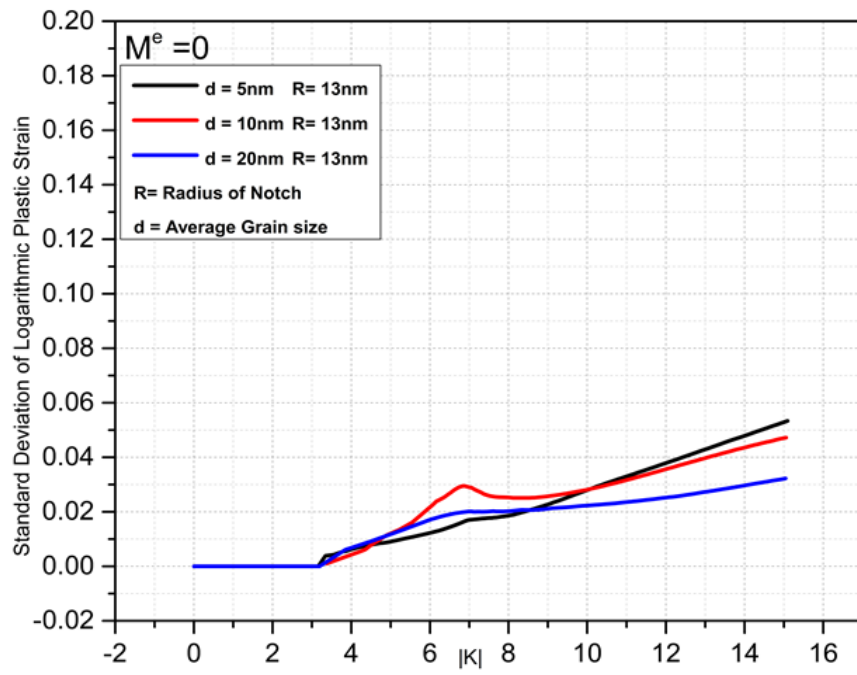


Fig. 21- Variation of Mean value of Logarithmic Plastic strain [$\log \lambda_1^p$] with increase in loading factor [|K|] for Average Grain Size [d] = 5, 10, 20 nm Notch Size [R] = 13 nm, and for corresponding M^e values



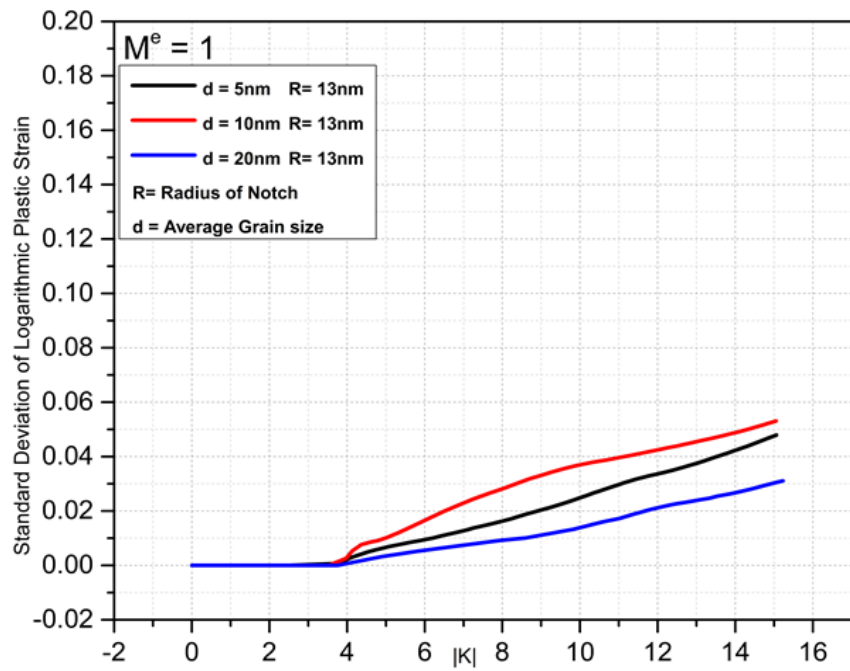
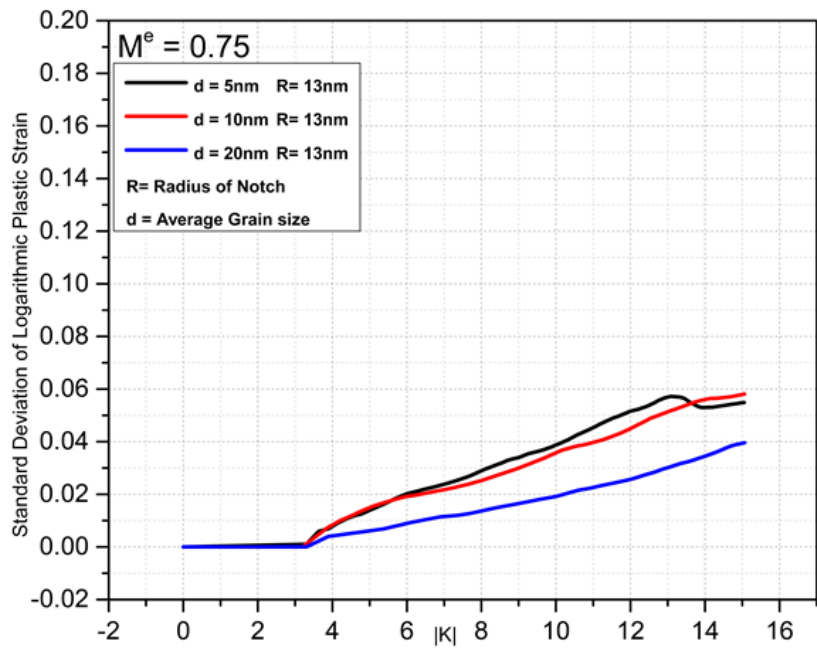


Fig. 22- Variation of Standard Deviation value of Logarithmic Plastic strain [$\log \lambda_1^p$] with increase in loading factor [|K|] for Average Grain Size [d] = 5, 10, 20 nm, Notch Size [R] = 13 nm, and for corresponding M^e values

The graphs of Mean value of Logarithmic Plastic Strain verses Effective loading rate ($|K|$) is as shown in fig. above. In the graph we can clearly observe that Mean value of $\log\lambda_1^p$ is very high for $R/d \approx 1$, very low for $R/d \gg 1$ and neither low nor very high for $R/d \ll 1$ for $M^e = 0.75, 1$. The Mean and Standard deviation value of $\log\lambda_1^p$ is almost remain unchanged upto loading rate of 3. For $M^e = 0, 0.25$ Mean value of $\log\lambda_1^p$ is increasing upto 7 then it is consolidating between 7 to 9 and again increasing beyond loading rate of 9. After loading rate of 9 in case of $M^e = 0, 0.25$ same trend we can observe which is as R/d is increasing Mean value of $\log\lambda_1^p$ is decreasing at given loading rate.

The graphs of Standard deviation value of Logarithmic Plastic Strain verses Effective loading rate ($|K|$) is as shown in fig. above. . If the value of standard deviation is very high or low, it is indicating that pattern of Logarithmic Plastic Strain inside the shear band near or away from notch is heterogeneous or homogeneous respectively.

From the graph standard deviation value is somewhat high for $R/d \approx 1$, very low for $R/d \gg 1$ and neither low nor very high for $R/d \ll 1$ respectively for $M^e = 0, 0.75, 1$. In case of $M^e = 0.25$ we can observe same trend for standard deviation as like Mean value of $\log\lambda_1^p$.

Chapter-6

Conclusion and future work

6.1 Conclusion-

- ❖ As the mode mixity value is increasing the size of plastic zone is decreasing.
- ❖ As R/d ratio is increasing the volume fraction in yielding is decreasing in case of Effect of Notch size and almost remains constant in case of Effect of Grain size.
- ❖ Diffused shear band pattern is observed in the Nanoglass.
- ❖ The rotation of shear band pattern is gets more visible for $M^e = 0.75$ in all cases.
- ❖ Some of the Shear bands develop in lower lobe of Notch particularly for $M^e = 0, 0.25$.
- ❖ Mean value of Logarithmic Plastic Strain [$\log \lambda_1^p$] is increasing as the mode mixity value is increasing in both Effect of Notch and Grain size cases.
- ❖ Standard deviation value of [$\log \lambda_1^p$] comparatively high for $M^e = 0$ for almost all cases which indicating that pattern of Logarithmic Plastic Strain inside the shear band near or away from notch is heterogeneous.

6.2 Future work

The goal of this research is to better understand how the fracture deformation takes place in Nanoglass structures. The findings of this study may give the required background for future research in this area. The following are some of specific studies to consider.

- ❖ In this study all the results of deformation in Nanoglass is investigated by Fracture simulation in Abaqus software. In future, this study or results can be verify and validate experimentally.

- ❖ In this study all the fracture simulation are carried up to only effective loading rate ($|K|$) of 15, in future the simulations can do beyond 15 to understand the behaviour of Notch surface deformation.

References

1. SS Hirmukhe, AT Joshi, I Singh (2022), Mixed mode (I and II) fracture behavior of nanoglass and metallic glass, *Journal of Non-Crystalline Solids* 580, 121390. (doi.org/10.1016/j.jnoncrysol.2021.121390)
2. Herbert Gleiter (2013), Nanoglasses: a new kind of noncrystalline materials, *Beilstein J. Nanotechnol.* 2013, 4, 517–533. (doi:10.3762/bjnano.4.61)
3. Anand L. and Su C. (2005), A theory for amorphous viscoplastic materials undergoing finite deformations, with application to metallic glasses, *Journal of the Mechanics and Physics of Solids*, 53(6), 1362-1396 (doi.org/10.1016/j.jmps.2004.12.006).
4. Anand L., Su C. (2007), A constitutive theory for metallic glasses at high homologous temperatures, *Acta Materialia*, 55, 3735-3747 (doi.org/10.1016/j.actamat.2007.02.020).
5. Franke O., Leisen D., Gleiter H., Hahn H. (2014), Thermal and plastic behavior of nanoglasses, *Journal of Materials research*, 29, 1210-1216 (doi.org/10.1557/jmr.2014.101).
6. Tandaiya P., Narasimhan R., Ramamurty U. (2007), Mode I crack tip fields in amorphous materials with application to metallic glasses, *Acta Materialia*, 55,6541-6552 (doi.org/10.1016/j.actamat.2007.08.017).
7. Tandaiya P., Ramamurty U., Ravichandran G., Narasimhan R. (2008), Effect of poisson's ratio on crack tip fields and fracture behavior of metallic glasses, *Acta Materialia*, 56,6077-6086 (doi.org/10.1016/j.actamat.2008.08.018).
8. Tandaiya P., Ramamurty U., Narasimhan R. (2009), Mixed mode (I and II) crack tip fields in bulk metallic glasses, *Journal of the Mechanics and Physics of Solids*, 57, 1880-1897 (doi.org/10.1016/j.jmps.2009.07.006).
9. Tandaiya P., Ramamurty U., Narasimhan R. (2011), On numerical implementation of anisotropic elastic-viscoplastic constitutive model for

- bulk metallic glasses, *Modelling and Simulation in Materials Science and Engineering*, 19, 015002 (doi.org/10.1088/0965-0393/19/1/015002).
10. Sha Z. D., He L. C., Pei Q. X., Pan H., Liu Z. S., Zhang Y. W., Wang T. J. (2014), On the notch sensitivity of CuZr nanoglass, *Journal of Applied Physics*, 115, 163507 (doi.org/10.1063/1.4873238).
 11. Wang X. L., Jiang F., Hahn H., Li J., Gleiter H., Sun J., Fang J. X. (2015), Plasticity of a scandium-based nanoglass, *Scripta Materialia*, 98, 40-43 (doi.org/10.1016/j.scriptamat.2014.11.010).
 12. Thamburaja P., Ekambaram R. (2007), Coupled thermo-mechanical modelling of bulkmetallic glasses: Theory, finite-element simulations and experimental verification, *Journal of the Mechanics and Physics of Solids*, 55, 1236-1273 (doi.org/10.1016/j.jmps.2006.11.008).
 13. Ivanisenko Y., Kubel C., Nandam S. H., Wang C., Mu X., Adjaoud O., Albe K., Hahn H. (2018), Structure and properties of nanoglasses, *Advanced Engineering Materials*, 20,1800404 (doi.org/10.1002/adem.201800404).
 - Anand L. and Su C. (2005), A theory for amorphous viscoplastic materials undergoing finite deformations, with application to metallic glasses, *Journal of the Mechanics and Physics of Solids*, 53(6), 1362-1396 (doi.org/10.1016/j.jmps.2004.12.006).
 14. Tandaiya P., Narasimhan R., Ramamurty U. (2013), On the mechanism and the length scales involved in the ductile fracture of a bulk metallic glass, *Acta Materialia*, 61, 1558-1570 (doi.org/10.1016/j.actamat.2012.11.033).
 15. Singh I., Narasimhan R., Zhang Y. W. (2014), Ductility enhancement in nanoglass: role of interaction stress between flow defects, *Philosophical Magazine Letters*, 94, 678-687 (doi.org/10.1080/09500839.2014.961584).
 16. Singh I., Narasimhan R. (2016), Notch sensitivity in nanoscale metallic glass specimens: insights from continuum simulations, *Journal of the*

Mechanics and Physics of Solids, 86, 53-69
(doi.org/10.1016/j.jmps.2015.10.001).

17. Ramamurty U., Jana S., Kawamura Y., Chattopadhyay K. (2005), Hardness and plastic deformation in a bulk metallic glass, *Acta Materialia*, 53, 705-717 (doi.org/10.1016/j.actamat.2004.10.023).
18. Abaqus 2017, Theory manuals, Version 6.5. Hibbit, Karlsson and Soresen Inc., RI, USA.